CHARLES UNIVERSITY IN PRAGUE

FACULTY OF SCIENCE

DEPARTMENT OF GENETICS AND MICROBIOLOGY

MASTER'S THESIS

Dissection of eIF3 functional domains promoting the 48S pre-initiation complex assembly

Petra Beznosková

Prague 2012

Supervisor: Leoš Valášek, Ph.D.

With this, I declare that I have written this work on my own, appropriately acknowledged citations, and used no other than the listed resources and aids.

.....

Petra Beznosková

Acknowledgement

I would like to thank my supervisor, Leoš Valášek Ph.D., for his patient guidance which allowed me to conduct this thesis.

I would like to thank Jon R. Lorsch Ph.D. and members of his laboratory for their help and guidance, namely to Colin E. Aitken.

I would also like to thank all members of LRGE laboratory, namely to Lucie Cuchalová, Sláva Gunišová, Anna Herrmannová, Martina Janošková, Tomáš Kouba, Olga Krýdová, Vanda Munzarová and Susan Wagner, for their help and advice that I have been given and for making my time in the lab enjoyable.

Last but not least, I would like to thank my family and my friends for their endless support during my studies.

Financial support:

This research was supported by The Wellcome Trusts Grant 090812/B/09/Z.

Abstract

In eukaryotes, translation initiation is guided by up to twelve protein initiation factors (eIFs) and begins with the formation of the 43S pre-initiation complex (PIC) composed of the small ribosomal subunit (40S), eIF2.GTP/Met-tRNA$_i^{Met}$ ternary complex, and eIFs 1, 1A, 3 and 5. The 43S PIC subsequently interacts with the 5′end of an mRNA (an mRNA recruitment step) and thus formed 48S PIC travels in 5′ to 3′ direction along the mRNA leader sequence to locate the AUG start codon (this presumably linear movement is generally known as scanning). Start site selection results in the dissociation of the initiation factors and joining of the large (60S) ribosomal subunit to form the 80S initiation complex poised for elongation. Eukaryotic initiation factor 3 (eIF3) plays a critical role in most of these events; however, the molecular details of most of its contributions are still unknown to us. Previous *in vivo* studies generated numerous mutations in all eIF3 subunits with specific defects either in the PICs assembly or in the following steps such as scanning, AUG recognition, etc. To understand the exact role of eIF3 in this intriguing process at the molecular level, we have embarked on a study that aims to dissect the individual functions of each eIF3 subunit in translation initiation using the purified mutant eIF3 complexes in the *in vitro* reconstitution system featuring several functional assays. Based on our preliminary results with some eIF3a/TIF32 , b and c mutants here we show that at least two of these *in vitro* assays, namely the 43S formation and mRNA recruitment protocols, are able to reveal and "measure the extent" of particular mechanistic effects of distinct eIF3 mutants.

Key words: translation initiation; mRNA recruitment, eIF3; PRT1; NIP1

Table of Contents

List of Abbreviations **8**

Introduction **10**

Review of previous research **12**

1. General translation initiation in Eukaryotes **12**

2. Eukaryotic initiation factor 3 (eIF3) **13**

2.1. Subunit composition and structure 13

2.2. The general roles of eIF3 in translation and beyond 15

2.3. The eIF3 role in the 43S PIC assembly process – predicted position of eIF3 on the small subunit 16

2.4. The eIF3 role in mRNA recruitment 18

3. Selected eIF3 subunits with a potential to influence the mRNA recruitment step **19**

3.1. The PRT1 subunit 19

3.2. The NIP1 subunit 22

Material and methods **24**

4. Laboratory equipment **24**

4.1. Centrifuges 24

4.2. Electrophoresis 24

4.3. Other equipment 24

5. Chemicals **25**

6. Solutions **27**

7. *Saccharomyces cerevisiae* strains **28**

8. *Escherichia coli* strain **29**

9. Plasmids **30**

10. Oligonucleotides **31**

11. Cultivation media **31**

11.1. Bacterial cultivation media and plates 31

11.2. Yeast cultivation media and plates 32

12. Bacterial and yeast cultivation **33**

12.1. Bacterial cultivation 33

12.2. Yeast cultivation 33

12.3. Permanent strain collections 33
12.4. Doubling time calculation 33
13. DNA manipulation 33
13.1. Plasmid DNA isolation – GenElute™ HP Plasmid Miniprep Kit (Sigma) 33
13.2. DNA modifications 35
13.3. Agarose gel electrophoresis 35
13.4. Isolation of DNA from the gel - QIAEX®II Gel extraction Kit (Qiagen) 35
13.5. Polymerase chain reaction (PCR) 36
13.6. Sequencing 37
13.7. Introducing DNA into target cells 37
13.7.1. Transformation of *E. coli* by electroporation method 37
13.7.2. Transformation of *E. coli* by heat-shock method 38
13.7.3. Transformation of *S. cerevisiae* by LiAc transformation method 38
14. Protein manipulation 39
14.1. WCE preparation for analysis by Western blotting 39
14.2. SDS-PAGE 39
14.3. Western Blotting 40
14.4. Chemiluminiscent detection 40
14.5. Gel blue staining 40
15. Purification of His-tagged eIF3 from *S. cerevisiae* (modified Acker et al. 2007) 41
15.1. Cultivation and concentrating for eIF3 purification 41
15.2. Grinding frozen yeast droplets using FreezerMill 6870 41
15.3. Sample preparation and column loading 42
15.4. Concentrator protocol 43
15.5. Fresh phosphocellulose column preparation (~10 mL) 44
15.6. Stripping HiTrap HP column 44
15.7. Bradford assay – protein quantitation 44
15.8. Nuclease contamination control 45
16. 43S gel shift assay (modified Acker et al. 2007) 45
16.1. Acrylamide gel for the 43S gel shift assay 45
16.2. 43S gel shift reaction 46
17. mRNA recruitment assay 47
17.1. Acrylamide gel for the mRNA recruitment assay 47

17.2. mRNA recruitment reaction 48
17.3. Hot capping of mRNA *RPL41A* 49
Results 50
18. Preparation of mutant eIF3 complexes for its testing in *in vitro* assays 50
18.1. Construction of recombinant vectors used for overexpression of all five eIF3 subunits 50
18.2. Preparation of yeast strains 51
18.3. Phenotypical control 54
19. Purification protocol of mutant eIF3 complexes 56
19.1. Yeast cell lysate preparation 57
19.2. Purification of mutant eIF3 complexes from the cell lysate 58
20. Effects of *PRT1* and *NIP1* mutations on eIF3 binding to the 40S ribosomes *in vitro* 61
20.1. The C-terminal truncation of NIP1 in *nip1-Δ60* does not change the binding affinity of the mutant eIF3 complex to the 43S PIC 61
20.2. The *PRT1* mutations disrupt the 43S PIC formation 63
21. The C-terminal truncation of NIP1 in *nip1-Δ60* does not affect the mRNA recruitment. 64
22. The *prt1-1* mutation reduces the efficiency but not the rate of mRNA recruitment to 43S PICs *in vitro* 66
Discussion 68
Conclusion 71
References 72

List of Abbreviations

APS	Ammonium persulfate
A-site	aminoacyl tRNA binding site
ATP	adenosine triphosphate
β-ME	β-mercaptoethanol
CTD	C-terminal domain
ddH_2O	double distilled water
dH_2O	distilled water
dsDNA	double strand DNA
DTT	Dithiothreitol
E. coli	*Escherichia coli*
EDTA	ethylenediaminetetraacetic acid
eIF	eukaryotic initiation factor
GDP	guanosine diphosphate
GDPNP	a non-hydrolyzable analog of GTP
GTP	guanosine triphosphate
HEPES	N-(2-Hydroxyethyl) piperazine-N-2-ethan sulfonic acid
LiAc	Lithium acetate
Met-$tRNA_i^{Met}$	methionyl initiator tRNA
MFC	multi factor complex
mRNA	messenger RNA
NMR	nuclear magnetic resonance
NTD	N-terminal domain
OD_{600}	optical density at 600 nm
PABP	poly A binding protein
PEG	polyethylene glycol
Pi	inorganic phosphate
PIC	pre-initiation complex
PMSF	phenylmethylsulfonyl fluoride
P-site	peptidyl-tRNA binding site
RRM	RNA recognition motif
S. cerevisiae	*Saccharomyces cerevisiae*
SAM	S-Adenosylmethionine
SDS	sodium dodecyl sulfate
Slg-	slow growth
TBE	Tris/Borate/EDTA
TBS	Tris-buffered Saline
TC	ternary complex

TEMED	Tetramethylethylenediamine
TG	Tris-Glycine
Tris	Tris(hydroxymethyl)-aminomethane
tRNA	transfer RNA
Ts-	temperature sensitivity
UTR	untranslated region
wt	wild-type
5´FOA	5-Fluoroorotic Acid

Introduction

Canonical translation initiation ensures timely and spatially coordinated formation of the trimeric complex between the 40S small ribosomal subunit (40S subunit), initiator Met-tRNA$_i^{Met}$ and an mRNA at its extreme 5' end, and concludes with the assembly of an elongation-competent 80S ribosome at the authentic AUG start codon. The entire process is orchestrated by numerous eukaryotic initiation factors (eIFs) with eIF3 representing the most intricate factor. The multiple essential roles of eIF3 during initiation include stabilization of eIF2/GTP/Met-tRNA$_i^{Met}$ ternary complex (TC) binding to 40S subunits, recruitment of 5'-^{7m}G capped mRNAs to 40S subunits, assistance in scanning of the 5' untranslated region (5' UTR) of the mRNA, and finally in aiding AUG initiation codon recognition. How does eIF3 promote all these steps mechanistically at the molecular level is not known and requires systematic investigation in a well defined system where all initiation steps can be clearly separated from each other and followed individually.

Laboratory of Professor Jon Lorsch Ph.D. at the Johns Hopkins School of Medicine in Baltimore has developed such a unique reconstituted system of yeast translation initiation, where particular initiation steps can be studied using purified factors. For example, this system enables to analyze the effects of the selected factors and their mutations on both the extent and kinetics of mRNA recruitment to the PIC in the so called mRNA recruitment assay. With this new approach they already showed that wild-type eIF3 complex is critically required for binding of natural mRNAs to the PIC *in vitro*, independent of its another critical role that precedes this step; i.e. an enhancement of TC binding to 40S ribosomes (Mitchell et al., 2010).

To find out what subunits of eIF3 (or even better their particular domains) ensure this critical role of the PIC assembly, we have started examining effects of various mutant eIF3 complexes in the aforementioned mRNA recruitment assay. In this thesis I present the first analysis of this kind using three different mutant eIF3 complexes that were selected based on 1) our knowledge of their *in vivo* phenotypes and 2) the feasibility of their construction. To be able to test their effect on the mRNA recruitment *in vitro*, I had to learn a variety of molecular biology, genetic and biochemical

techniques that are all carefully described below. I should also note here that the preparation of plasmids and strains was carried out at my home lab at the Institute of Microbiology ASCR, whereas the purification of eIF3 complexes from the budding yeast *Saccharomyces cerevisiae* and all *in vitro* experiments presented here were performed at the laboratory of Professor Jon Lorsch Ph.D. (Johns Hopkins University School of Medicine; under the supervision of Colin E. Aitken), where I spent two months during summer 2011.

Review of previous research

1. General translation initiation in Eukaryotes

Translation can be divided into four phases: initiation, elongation, termination and ribosome recycling. During the initiation phase the functional translational complex is established. First the 40S ribosome with several initiation factors assemble on mRNA with the initiator Met-tRNA$_i^{Met}$ placed in the P site and the whole pre-initiation complex then starts searching for the AUG initiating codon. Upon AUG selection, the 80S initiation complex is formed and the next stage – elongation – begins, during which a protein encoded by a given mRNA is being efficiently synthesized, until the STOP codon appears in the ribosomal A-site triggering termination. Controlled by eukaryotic release factors (eRFs), the peptide is released and after that the ribosomal subunits, deacetylated tRNA in the P-site and mRNA are recycled.

Translation initiation is the first and the most regulated the protein synthesis process, orchestrated by numerous proteins and three protein complexes called eukaryotic initiation factors (eIFs). It starts, when the initiator methionyl tRNA (Met-tRNA$_i^{Met}$) binds to eIF2 in its GTP form and forms the so called ternary complex (TC). Then the multiprotein eIF3 complex, together with eIFs 1, 1A and 5 promotes TC recruitment to the small ribosomal subunit (40S) producing the 43S pre-initiation complex (PIC) (Jackson et al., 2010) which binds to the very 5´end of a capped mRNA pre-bound with eIF4F, eIF4B and the poly-A binding protein (PABP) (Marintchev and Wagner; Sachs and Varani, 2000). In more detail, to form the 48S PIC, eIFs 1 and 1A, after formation of the 43S PIC stabilize a specific 40S conformation that opens the mRNA binding channel for mRNA loading. That requires dissolving the latch formed by helices 18 (h18) and 34 (h34) of 18S rRNA and establishing a new interaction between RPS3 and h16 (Passmore et al., 2007). This conformation of 40S is called open - scanning permissive. The newly established 48S PIC then scans the 5' UTR of mRNA until it recognizes the first AUG codon. During the scanning process eIF2 partially hydrolyzes the GTP stimulated by eIF5, but the posphate (Pi) is not released until the Met-tRNA$_i^{Met}$ base-pairs with the AUG start codon. After that eIF1 dissociates and as a

result the free Pi is released and the 48S PIC undergoes a reciprocal conformational change to the closed state arresting scanning. It allows joining of the large ribosomal subunit (60S) stimulated by eIF5B (Pestova et al., 2000) accompanied by dissociation of all initiation factors except of eIF1A (Unbehaun et al., 2004) and eIF3 (Szamecz et al., 2008). Upon GTP hydrolysis by eIF5B, the 80S initiation complex is formed and ready for the next step - elongation.

For the new initiation cycle, the eIF2.GDP recycling is crucial. Dissociated eIF2.GDP has to be exchanged back into its GTP form in order to bind the initiator Met-$tRNA_i^{Met}$ again. This exchange is executed by the eIF2B factor (Pavitt et al., 1998; Krishnamoorthy et al., 2001; Fabian et al., 1997).

2. Eukaryotic initiation factor 3 (eIF3)

Eukaryotic initiation factor 3 (eIF3) is the protein complex that was originally identified at the end of the seventies, but it was not until the recent 15 years that it has begun receiving the experimental attention that it certainly deserves. During these years it has been shown that eIF3 plays multiple essential roles in general translation across all eukaryotic species.

2.1. Subunit composition and structure

eIF3 as the largest initiation factor with the molecular mass of about 550kDa in yeast (Naranda et al., 1994) and 650kDa in mammals (Behlke et al., 1986) is a multiprotein complex.

The eIF3 subunit composition in yeast and mammals dramatically differs. Whereas human eIF3 consists of 13 non-identical subunits, designated in alphabetical order as eIF3a-m (Damoc et al., 2007; Unbehaun et al., 2004; Zhou et al., 2008), in budding yeast eIF3 contains only five essential stoichiometric core subunits (TIF32, PRT1, NIP1, TIF34 and TIF35), which are orthologs to human eIF3a, b, c, g and i, and the substoichiometric HCR1 with a human homologue eIF3j (Phan et al., 1998; Asano et al., 2001) (Fig. 1). Whereas the subunit interaction map of the yeast eIF3 core has been known since the beginning of this millennium, the true composition of the core of mammalian eIF3 remains unclear. One study suggests that the eIF3g and eIF3i subunits, which are evolutionarily conserved between human and the yeast *Saccharomyces cerevisiae*, are dispensable for active mammalian eIF3 complex formation and that three

evolutionarily conserved subunits (eIF3a, eIF3b, and eIF3c) and three non-conserved subunits (eIF3e, eIF3f, and eIF3h) comprise the functional core of mammalian eIF3 (Masutani et al., 2007). However, other work based on tandem mass spectrometry and solution disruption assays identified three stable modules instead, one of which, composed of a, b, i, and g subunits, closely resembled the yeast eIF3 core (Zhou et al., 2008).

Unfortunately, despite an enormous effort by many groups, the structure of neither yeast nor mammalian eIF3 has been solved as yet. Until a real structure is known, at least a three-dimensional model of the MFC based largely on binary interactions between isolated subunit was established (Valášek et al., 2002). Based on recent structural analysis of at least some individual eIF3 subunits, this model has been recently reshaped to incorporate these new structures into the whole image of the MFC. In particular, the NMR structures of the interaction between the RRM of human eIF3b and the N-terminal peptide of human eIF3j (Elantak et al., 2010) and of the C-terminal RRM of human eIF3g (Cuchalová et al., 2010), the X-ray structure of the yeast TIF34-PRT1 complex (Herrmannová et al., 2011), and finally the 3D structural model of the NIP1-PCI domain (Kouba et al., 2011) used to replace the original schematic representations of the corresponding molecules (see Fig. 1).

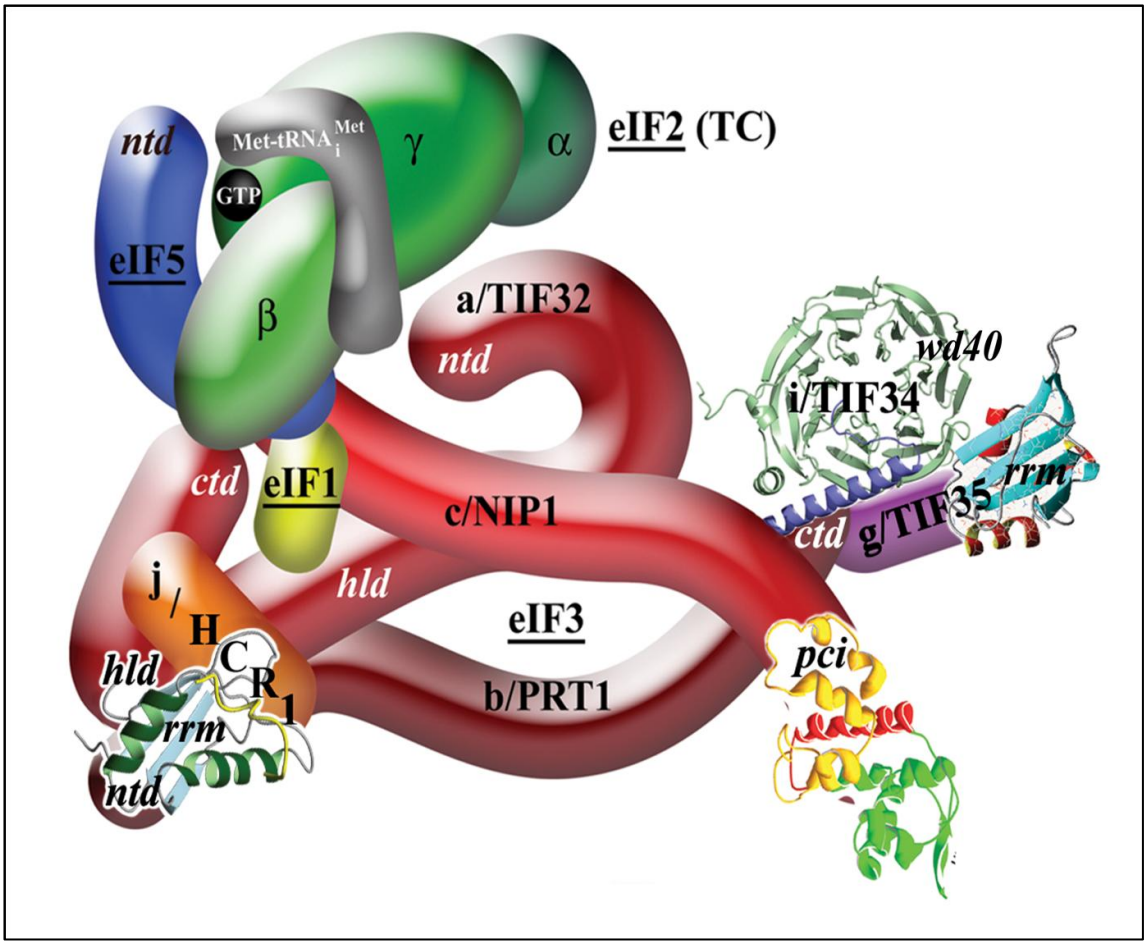

Figure 1. A revised 3D model of eIF3 and its associated eIFs in the MFC (based on the data from (Valášek et al., 2002); ntd, N-terminal domain; ctd, C-terminal domain; hld, HCR1-like domain; rrm, RNA recognition motif; TC, ternary complex). The NMR structure of the interaction between the RRM of human eIF3b (green and light blue) and the N-terminal peptide of human eIF3j (yellow) (Elantak et al., 2010), the NMR structure of the C-terminal RRM of human eIF3g (red and sky-blue) (Cuchalová et al., 2010), and the X-ray structure of the yeast TIF34–PRT1 complex (Herrmannová et al., 2011), and the 3D structural model of the NIP1-PCI domain (Kouba et al., 2011) were used to replace the original schematic representations of the corresponding molecules.

2.2. The general roles of eIF3 in translation and beyond

As for the eIF3 functions in general, historically, eIF3 has been first implicated in the formation of the 43S and 48S PICs in mammalian *in vitro* systems made of reticulocyte lysates (Trachsel and Staehelin, 1979; Trachsel et al., 1977; Benne and Hershey, 1978). Later on the same functions were also demonstrated in budding yeast

(Phan et al., 1998, 2001). And yeast eIF3 has also been implicated in scanning and AUG recognition (Nielsen et al., 2004; Valášek et al., 2004), making the budding yeast an excellent model system to study the functions of eIF3 in initiation in great detail. One of the key, still unanswered questions is which part(s) of eIF3 is(are) responsible for execution of which translational step.

eIF3 is not involved only in canonical translation initiation. It was also implicated in regulation of protein synthesis during viral infection (Guo et al., 2000), newly in cellular defense against the HIV infection (Jäger et al., 2012), in mRNA surveillance by nonsense-mediated decay pathway (NMD)(Isken et al., 2008), in signal transduction pathways by recruiting protein kinases such as mTORC1 and S6K to surface of 40S subunit (Harris et al., 2006; Holz et al., 2005), and in the gene-specific translational control mechanism termed reinitiation (REI) in yeast, plant and mammalian cells (Munzarová et al., 2011; Szamecz et al., 2008; Park et al., 2001; Pöyry et al., 2007).

2.3. The eIF3 role in the 43S PIC assembly process – predicted position of eIF3 on the small subunit

It has been suggested that for the first initiation step; i.e. the 43S PIC assembly, there are two major ways of how the eIFs associate with ribosomes. The first one, the "stochastic – prokaryotic-like" pathway assumes that the eIFs bind to the ribosome on the individual basis, one by one. The other "higher order-eukaryotic" pathway postulates the existence of the multifactor complex (MFC), where the eIFs 1, 3, 5 with TC can bind 40S ribosome as a pre-organized unit (Asano et al., 2000), which seems to be the more efficient pathway of factor recruitment to the ribosome especially upon growth permissive conditions (Valášek et al., 2004, 2002; Nielsen et al., 2004, 2006; Jivotovskaya et al., 2006; Yamamoto et al., 2005; Elantak et al., 2010; Cuchalová et al., 2010; Chiu et al., 2010; Mitchell et al., 2010).

To better understand the molecular details of the eIF3 role in the PIC assembly process, a systematic mapping of the positions of specific domains of various eIF3 subunits on the 40S has begun. It was shown, that the extreme N-terminal domain (NTD) of TIF32 forms a crucial intermolecular bridge between eIF3 and the 40S by interacting with small ribosomal protein RPS0 in the vicinity of the mRNA exit pore (Szamecz et al., 2008). In addition, deleting the C-terminal domain (CTD) of TIF32

reduced the MFC association with the 40S when the connection between eIF3 and eIF5/TIF5 in the MFC was impaired by the tif5-7A mutation (Valášek et al., 2003); and the TIF32-CTD was found to interact with helices 16–18 of 18S rRNA (16) and RPS2 and RPS3 (Chiu et al., 2010). NIP1-CTD was shown to interact with ASC1/RACK1 and also with RNA (Kouba et al., 2011). RPS2 is also known to interact with the CTD of HCR1(Elantak et al., 2010; Chiu et al., 2010). The TIF35 subunit interacts with the 40S beak proteins RPS3 and RPS20 (Cuchalová et al., 2010) and consistently, although not expected, recently work by Herrmannova et al. showed that TIF35 together with another small eIF3 subunits in TIF34 does stabilize eIF3 association with the PICs *in vivo* (Herrmannová et al., 2011). These interactions allowed us to propose that yeast eIF3 associates with the solvent-exposed side of the 40S subunit (see the model in Fig. 2), as others have proposed for mammalian eIF3 (Siridechadilok et al., 2005). By wrapping around the neck of the back of the 40S subunit, eIF3 may serve as a bridge between components bound near the mRNA entry and exit channels and coordinate not only the assembly of the PIC but also roles of all involved eIFs in the subsequent initiation steps. Consistent with this, a recent study employing a chemical footprinting and UV-crosslinking observed direct interactions between mammalian eIF3 and mRNA at both entry and exit channels of the PIC (Pisarev et al., 2008).

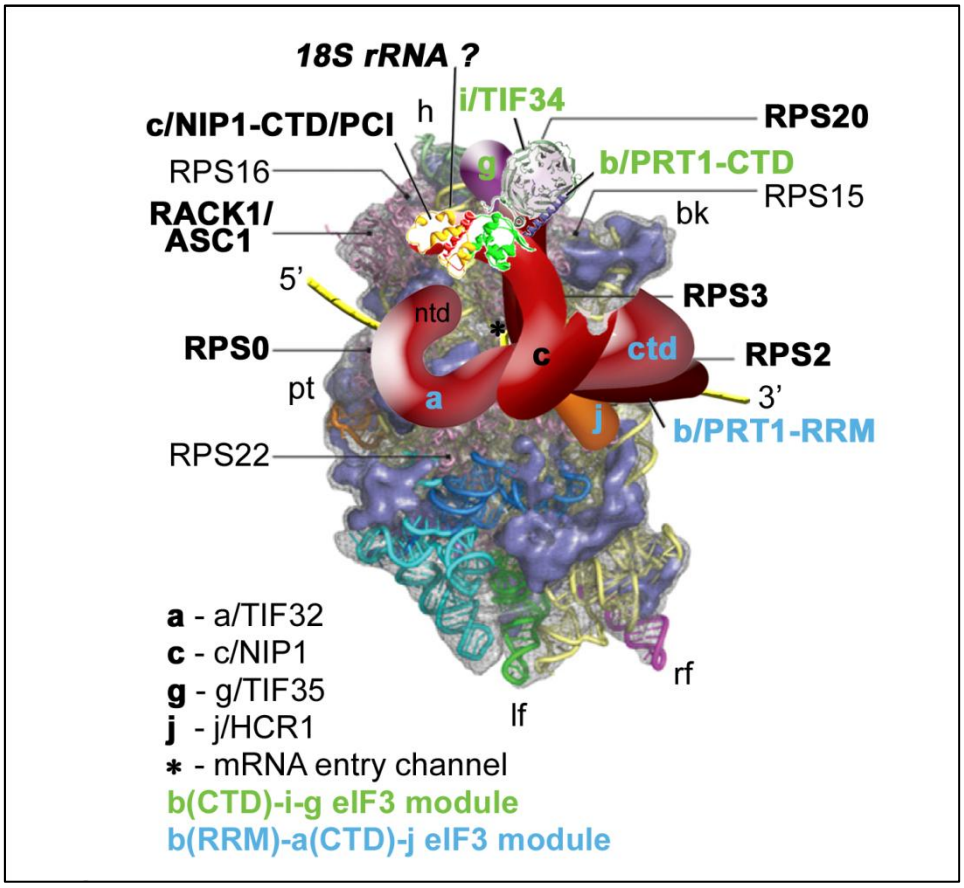

Figure 2. Hypothetical location of *S. cerevisiae* eIF3 (Kouba et al., 2011) on the back side of the 40S subunit based on the data presented, including the interactions between NIP1-CTD and ASC1 (and potentially also with 18S rRNA), RPS0 and TIF32-NTD, RPS2 and j/ HCR1, RPS2 and 3 and TIF32-CTD, helices 16–18 of 18S rRNA and TIF32-CTD, and RPS3 and 20 and TIF35 (see text for further details). The 3D structural model of the NIP1-PCI domain determined in this study was used to replace the original schematic representation of the same molecule. The yellow lines represent mRNA.

2.4. The eIF3 role in mRNA recruitment

The 43S PIC is recruited to the 5´ end of an mRNA via the 7-methylguanosine cap structure. The 5´ cap is bound by eIF4E, a component of the trimeric cap-binding complex eIF4F. eIF4F also contains the DEAD box RNA helicase eIF4A and a multidomain protein, eIF4G that interacts with a number of other factors and RNA. These interactions are thought to be critical for mRNA recruitment at least in mammalian systems (Asano et al., 2001; He et al., 2003; Korneeva et al., 2000; Lamphear et al., 1995). In mammals, it has been shown that eIF4G interacts with eIF3,

and this interaction also seems to stimulate binding of activated mRNP to the 43S PIC by a great deal (LeFebvre et al., 2006). On the contrary, in yeast it was shown that mRNA can be recruited to the ribosome in the absence of eIF4G suggesting that alternative pathways are possible (Jivotovskaya et al., 2006). One possibility is that eIF5, which interacts with both eIF3 and eIF4G, serves to bridge the mRNP and 43S PIC complexes via eIF4G and eIF3 in yeast (Asano et al., 2001). Both mammalian and yeast eIF4B bind eIF3, and eIF4B is critical for loading of mRNA onto the PIC *in vitro* in both systems (Mitchell et al., 2010; Dmitriev et al., 2003; Méthot et al., 1996). Finally, eIF3 could be the critical factor as it was shown to possess RNA-binding affinity.

Indeed, eIF3 was only recently shown to strongly promote mRNA recruitment the PICs *in vitro*, independently of its enhancement of TC binding (Mitchell et al., 2010). This is consistent with the recent *in vivo* "degron" studies in yeast (Jivotovskaya et al., 2006), in which upon degradation of eIF3 binding of *RPL41A* mRNA to 43S complexes was dramatically reduced, whereas the loss of eIF4G led, conversely, to *RPL41A* mRNA accumulation in 43S PICs. The fact that eIF3 strongly enhanced the recruitment of an unstructured model mRNA with a long 5' leader, whereas recruitment of an mRNA with a short 5' leader but long 3' extension was less sensitive to eIF3 (Mitchell et al., 2010) further illustrates an active role of eIF3 in mRNA delivery to the ribosome in the 5' cap-dependent way.

3. Selected eIF3 subunits with a potential to influence the mRNA recruitment step

3.1. The PRT1 subunit

PRT1 is a subunit of eIF3 homologous to the mammalian p116 subunit with the molecular mass about 90kDa (Naranda et al., 1994). It was identified as a gene required for the initiation of protein biosynthesis in *Saccharomyces cerevisiae* by complementation of the temperature-sensitive *prt1-1* mutation (Keierleber et al., 1986), as the first translation initiation factor in yeast.

PRT1 is considered to be the major scaffolding subunit within the eIF3 complex in both yeast and mammals (Zhou et al., 2008; Fraser et al., 2004; Asano et al., 1998). In

budding yeast, PRT1 interacts with all other eIF3 subunits (Phan et al., 1998; Valášek et al., 2002; Valásek et al., 2001) (Fig. 3).

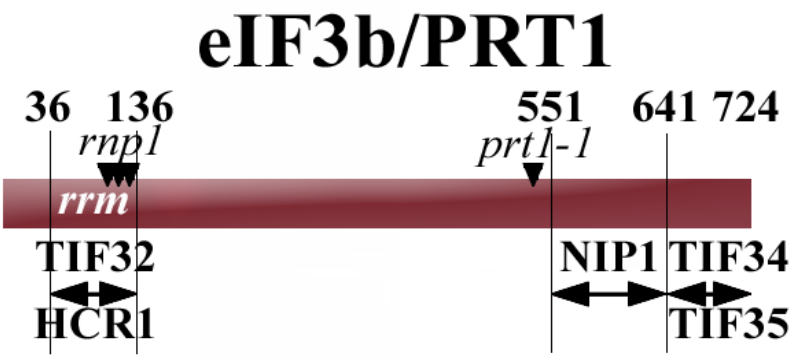

Figure 3. Schematic of PRT1 with arrows delimiting minimal binding domains for indicated proteins. RRM domain and positions of *rnp1* and *prt1-1* mutation are indicated.

PRT1 is the second largest eIF3 subunit and can be structurally divided into three parts with different binding partners. The NTD of PRT1 contains a conserved RNA recognition motif (RRM), which interacts simultaneously with HCR1 and with internal domain of eIF3 subunit TIF32 that has a sequence and functional similarity to HCR1 (Valásek et al., 2001; Elantak et al., 2010). The structure of this RRM was already solved for human and yeast eIF3 (ElAntak et al., 2007; Khoshnevis et al., 2010). It was shown that expression of a truncated form of PRT1 lacking the N-terminal RRM sequestered TIF34 and TIF35 in a defective subcomplex that could not stably associate with 40S ribosomes (Valásek et al., 2001).

Its middle domain was predicted to fold into two β-propeller structures (Marintchev and Wagner), the second of which contains a binding site for NIP1. The extreme α-helical CTD of the PRT1 scaffold is required for association of TIF34 and TIF35 subunits (Herrmannová et al., 2011; Asano et al., 1998)(see Figure 3 for schematic interaction map). PRT1 interacts with TIF34, which adopts a seven-bladed β-propeller structure made up of seven WD-40 repeats, via two contacts, one of which has an ionic and the other hydrophobic character (Fig. 1) (Herrmannová et al., 2011). TIF35 then interacts with TIF34 and PRT1 through its NTD containing a predicted Zn-finger domain via yet to be defined binding sites (Asano et al., 1998) (see the 3D model in Fig. 1).

As mentioned above, the NTD of PRT1 contains an RNA recognition motif (RRM). This putative RNA binding domain was an obvious region to mutate in the hope

of generating mutants that would implicate this part of eIF3 in mRNA recruitment by disrupting a PRT1-mRNA interaction. However, Met-$tRNA_i^{Met}$ or rRNA could also be binding partners of the PRT1-RRM. Furthermore, the RRM is located within the binding domain for HCR1 and TIF32 in PRT1 (Valásek et al., 2001), and these protein-protein interactions could be disrupted by mutation of the RRM. To better address the role of this only putative RNA-binding domain in PRT1, a multiple alanine substitution of its RNP1 motif was generated. This so called *rnp1* mutation was shown to produce a temperature sensitive (Ts-) phenotype by impairing the eIF3 recruitment to the 40S subunit *in vivo*, as the most probably major defect (Nielsen et al., 2006). This mutation changed a seven-residue RNP1 stretch (124 FLFVE130KG)(see Fig. 4) of a significant sequence similarity to the RNP1 motif of the second RRM domain in poly(A) binding protein (PABP) (Deo et al., 1999) to a stretch of seven alanines (Nielsen et al., 2006). Interestingly, the residues 124, 130, 126, and 128 correspond to amino acid residues that in human PABP make direct interactions with RNA through their side chains (Deo et al., 1999) suggesting that mutations at these positions in PRT1 could disrupt its putative interaction with RNA. Hence we picked this mutant as one of the first to analyze its effects in our *in vitro* assays described above.

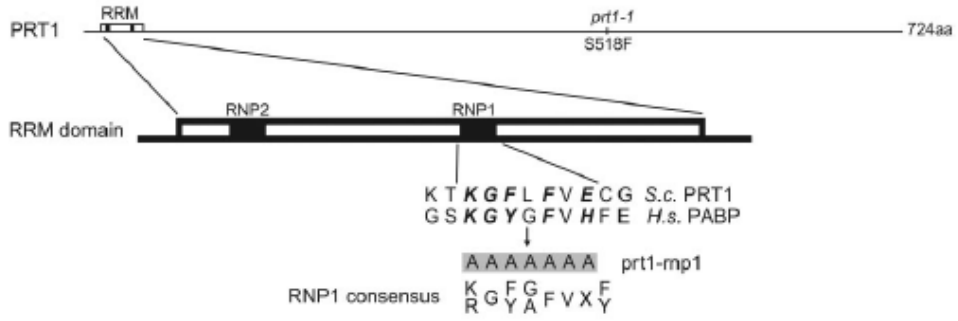

Figure 4: Schematic representation of PRT1, showing the location of *prt1-1*, the RRM domain, and the RNP1 and RNP2 motifs (Nielsen et al., 2006). Below is a sequence alignment of this region in yeast (*Saccharomyces cerevisiae*) PRT1 and residues in RRM2 of human PABP, together with the seven residues that are changed to alanines in *prt1-rnp1*. Letters in boldface indicate amino acids in PABP RRM2 that make direct contact with RNA (Deo et al., 1999).

Another mutant that we selected was the *prt1-1* mutation in the same eIF3 subunit. It is one of the original cell-cycle dependent mutants isolated by Hartwell et al. that leads to the temperature-sensitive growth and severe reduction in translation

initiation rates *in vivo* (Hartwell and McLaughlin, 1968). This mutation replaces Ser-518 with Phe and does not affect the eIF3 integrity (Phan et al, 2001). *In vitro* analysis of heat-inactivated *prt1-1* extracts revealed a defect in binding of TC to 40S ribosomal subunits that could be complemented with purified eIF3 complexes (Danaie et al., 1995; Phan et al., 1998) and binding of mRNA, eIFs 1 and 5 and eIF3 itself in these extracts (Phan et al., 2001). Later on a paper came out showing that TC and mRNA binding to 40S subunits is not diminished in *prt1-1* cells at the restrictive temperature *in vivo* (Nielsen et al., 2004).

3.2. The NIP1 subunit

The N-terminal domain of NIP1 makes direct contacts with eIFs 1 and 5, and via the latter also associates with the TC (Valášek et al., 2002; Asano et al., 2000), serving as a critical nucleation center for the MFC formation. The following domain then interacts with the PCI domain of TIF32 and, towards the C-terminus, NIP1 captures the triangle-like network of interactions among all three large subunits by binding to PRT1. In particular, residues 371-570 of NIP1 contain a binding site for PRT1 that is required for tight association of the PRT1-TIF34-TIF35 subcomplex with other eIF3 subunits (Valášek et al., 2002). The actual CTD is formed by a canonical PCI domain that interacts with RNA and is extended by extreme C-terminus, which directly interacts with blades 1–3 of the small ribosomal protein RACK1/ASC1, which is a part of the 40S head (Kouba et al., 2011)(see Fig. 5 for schematic interaction map). The nip1-Δ60 is the shortest viable NIP1-CTD truncation removing the last 60 amino acid residues forming the last α-helix, which is not a part of the PCI, and both terminal β-sheets of the PCI. It is not lethal and produces a slow growth (Slg-) phenotype that is slightly exacerbated at higher temperature (Kouba et al., 2011). Kouba showed that the initiation defect in the nip1-Δ60 mutant is by a large degree caused by a reduced rate of the 43S PIC formation and/or by its decreased stability *in vivo* (Kouba et al., 2011).

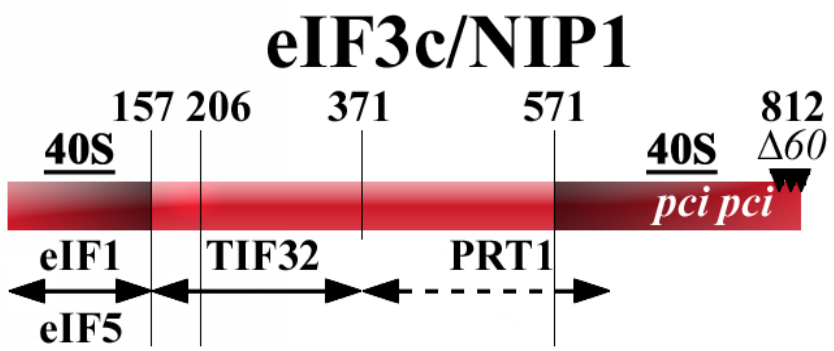

Figure 5. Schematic of NIP1 with arrows delimiting the minimal binding domains for the indicated proteins identified previously. The location of the PCI homology domain and position of a short C-terminal deletion (*Δ60*) are indicated.

Material and methods

4. Laboratory equipment

4.1. Centrifuges

Beckman Coulter Allegra® X-15R Centrifuge, rotor SX 4750A

Beckman Coulter optima^{TM}L-90K Ultracentrifuge, rotor SW 41

Biosan Centrifuge/vortex Multi Spin MSC-300

Eppendorf Centrifuge 5414D

Sorvall Centrifuge, rotor SS-34

4.2. Electrophoresis

Bio-Rad Mini-PROTEAN 3 cell

Bio-Rad Criterion Cell

Bio-Rad PowerPac Basic power supply

Bio-Rad PowerPac HC power supply

Bio-Rad PowerPac Universal power supply

4.3. Other equipment

ÄKTAfplc™ (GE Healthcare)

Amicon Ultra concentrator (Millipore, 10K MWCO)

Beckman Coulter DU®530 Life Science UV/VIS Spectrophotometer

BioComp Gradient Master

Bio-Rad Gene Pulser Xcell Electroporation System

Biosan Bio RS-24 Rotator

Biosan Mini Rocker MR-1

Biosan Multi RS-60 Rotator

Brandel BR-188 Density Gradient Fractionation System

Easy-load-Masterflex I/P TM (Millipore)

Eppendorf Mastercycler ep gradient S

Eppendorf Thermomixer Comfort

HiTrap HP column (GE Healthcare)

Multitron INFORS HT shaker

Pellicon 2 cassette 0.45μm (Millipore)

Pellicon Cassette Acrylic Holder (Millipore)

Scientific Industries Vortex genie 2

Superose 12 gel filtration column (GE Healthcare)

Syngene G:BOX iChemi – gel documentation and analysis system

5. Chemicals

10x TBE (Bio-Rad)

10x TBS (Bio-Rad)

10x TG (Bio-Rad)

40% Acrylamide:Bis-Acrylamide (19:1) (Sigma)

40% Acrylamide:Bis-Acrylamide (37.5:1) (Sigma)

Agar (Serva)

Aprotinin (Sigma)

APS (Sigma)

Bacto Peptone (Becton, Dickinson and Company)

Bacto Tryptone (Becton, Dickinson and Company)

Bacto Yeast Extract (Becton, Dickinson and Company)

Benzamidine (Sigma)

Bio-Rad Protein Assay Kit (Bio-Rad)

Bradford Reagent (Sigma)

Bromophenol Blue (Sigma)

Complete Protease Inhibitor Mix tablets (Roche)

Criterion Precast Gels, 4-20% Tris-HCl, 1mm, 12+2 Well Comb, 45 μl (Bio-Rad)

D-glucose (Lachner)

DNase (Roche)

DTT (Sigma)

ECLTM Anti Mouse IgG, HRP-linked whole antibody (from donkey) (GE Healthcare)

EDTA (Sigma)

EDTA-free Complete Protease Inhibitor Mix tablets (Roche)

Electroporation cuvettes (Eppendorf)

EP-MAXTM 10B Competent Cells (Bio-Rad)

Ethidium bromide (Serva)

GDPNP (MWG)

Gel Code® Blue Stain Reagent (Thermo Scientific)

HEPES (Serva)

Imidazole (Fluka)

Leupeptin (Sigma)

NTP (NEB)

PEG (Fluka)

Phosphocellulose (Whatman Co.)

PMSF (Serva)

RNA loading dye 2x (Fermentas)

RNase inhibitor (Roche)

SAM (NEB)

SC-LEU-TRP(Formedium)

SDS solution 20% (Sigma)

SeaKem® LE Agarose (Lonza)

Sigmacote (Sigma)

Subcloning EfficiencyTM DH5αTM Competent Cells (Invitrogen)

Sucrose (Fluka)

SuperSignal West Femto Maximum Sensitivity Substrate (Thermo Scientific)

TEMED (Sigma)

Tris (Serva)

Triton X-100 (Sigma)

Tween 20 (Sigma)

Urea (Sigma)

Vaccinia capping enzyme (NEB)

Xylene cyanol (Sigma)

[α^{32}P]GTP (MWG)

β-Mercaptoethanol (Sigma)

6. Solutions

B-200 buffer : 20 mM HEPES (pH 7.4); 200 mM KCl; 0.1 mM EDTA; 10% glycerol; 2 mM DTT

B-350 buffer : 20 mM HEPES (pH 7.4); 350 mM KCl; 0.1 mM EDTA; 10% glycerol; 2 mM DTT

B-1000 buffer : 20 mM HEPES (pH 7.4); 1 M KCl; 0.1 mM EDTA; 10% glycerol; 2 mM DTT

BB buffer: 20 mM Tris-HCl (pH 7.5); 100 mM KCl; 5 mM $MgCl_2$; 0,5 mM β-ME; 1mM PMSF; 20 mM imidazole; 10% glycerol; 1x EDTA-free Complete Protease Inhibitor Mix tablets

Blotting buffer (1000 mL for 1 blotting): 700 mL dH_2O; 200 mL methanol; 100 mL; 10xTG

Enzyme storage buffer: 20 mM HEPES (pH 7.4); 100 mM KOAc; 10% glycerol; 2 mM DTT

LiAc/TE 1x: 1 mM Tris-HCl; 0.1 mM EDTA; 10 mM Lithium acetate

Low imidazole buffer: 20 mM HEPES (pH 7.4); 350 mM KCl; 5mM $MgCl_2$; 10% glycerol; 20 mM imidazole; 10 mM β-ME

Low salt buffer: 20 mM HEPES (pH 7.4); 100 mM KCl; 0.1 mM EDTA; 10% glycerol; 2 mM DTT

High imidazole buffer: 20 mM HEPES (pH 7.4); 350 mM KCl; 5mM $MgCl_2$; 10% glycerol; 25 mM imidazole; 10 mM β-ME

Native gel dye: 50% sucrose; 0.02% bromophenol blue, 0.02% xylene cyanol

PEG/LiAc/TE: 1 mM Tris-HCl; 0.1 mM EDTA; 10 mM Lithium acetate; 50% PEG

Recon Buffer 10x: 300 mM HEPES•KOH; (pH 7.4); 1 M KOAc pH 7.6; 30 mM $Mg(OAc)_2$; 20 mM DTT

Sample buffer for agarose gel electrophoresis 6x: 30% glycerol; 0.25% bromophenol blue

Sample loading buffer for SDS-PAGE 4x: 1M Tris-HCl (pH 6.8); 40% glycerol; 8% SDS; 0.06% bromophenol blue; 1.47% β-ME

SDS-PAGE running buffer: 1xTG; 0.1% SDS

TBS-T buffer: 1x TBS; 0.1% Tween 20

THEM 10x: 340mM Tris Base, 570mM HEPES, 1mM EDTA, 25mM $MgCl_2$

7. *Saccharomyces cerevisiae* strains

Strain	Genotype	Source
H505	MATa ura3-52 trp1 leu2-del1 his3-del200 pep4::HIS3 prb1-del1.6R can1 GAL+	A. Hinnebusch
H507	MATa ura3-52 trp1 leu2-del1 his3-del200 pep4::HIS3 prb1-del1.6R can1 GAL+ tif32del::KanMX4 (YCpTIF32-His-U)	A. Hinnebusch
PBH42	MATa ura3-52 trp1 leu2-del1 his3-del200 pep4::HIS3 prb1-del1.6R can1 TIF35-del GAL+ (YEp-TIF35)	This study
PBH44	MATa ura3-52 trp1 leu2-del1 his3-del200 pep4::HIS3 prb1-del1.6R can1 prt1-del GAL+ (YEpPRT1-U)	This study
PBH50	MATa ura3-52 trp1 leu2-del1 his3-del200 pep4::HIS3 prb1-del1.6R can1 GAL+ tif32del::KanMX4 (YEpPRT1-His-TIF34-TIF35-W, YEpTIF32-NIP1-L)	This study

PBH51	MATa ura3-52 trp1 leu2-del1 his3-del200 pep4::HIS3 prb1-del1.6R can1 GAL+ tif32del::KanMX4 (YEpPRT1-His-TIF34-TIF35-W, YEptif32-Δ8-NIP1-His-L)	This study
PBH52	MATa ura3-52 trp1 leu2-del1 his3-del200 pep4::HIS3 prb1-del1.6R can1 prt1-del GAL+ (YEpPRT1-His-TIF34-TIF35-W, YEpTIF32-NIP1-L)	This study
PBH54	MATa ura3-52 trp1 leu2-del1 his3-del200 pep4::HIS3 prb1-del1.6R can1 prt1-del GAL+ (YEpprt1-rnp1-His-TIF34-TIF35-W, YEpTIF32-NIP1-L)	This study
PBH55	MATa ura3-52 trp1 leu2-del1 his3-del200 pep4::HIS3 prb1-del1.6R can1 prt1-del GAL+ (YEpprt1-1-His-TIF34-TIF35-W, YEpTIF32-NIP1-L)	This study
PBH56	MATa ura3-52 trp1 leu2-del1 his3-del200 pep4::HIS3 prb1-del1.6R can1 nip1-del GAL+ (YEpNIP1-His)	This study
PBH57	MATa ura3-52 trp1 leu2-del1 his3-del200 pep4::HIS3 prb1-del1.6R can1 tif34-del GAL+ (YEp-TIF34)	This study
PBH64	MATa ura3-52 trp1 leu2-del1 his3-del200 pep4::HIS3 prb1-del1.6R can1 nip1-del GAL+ (YEpPRT1-His-TIF34-TIF35-W, YEpTIF32-NIP1-L)	This study
PBH65	MATa ura3-52 trp1 leu2-del1 his3-del200 pep4::HIS3 prb1-del1.6R can1 nip1-del GAL+ (YEpPRT1-His-TIF34-TIF35-W, YEpTIF32-nip1-Δ60-L)	This study

8. *Escherichia coli* strain

Strain	Genotype	Source
DH5α	fhuA2 Δ(argF-lacZ)U169 phoA glnV44 Φ80 Δ(lacZ)M15 gyrA96 recA1 relA1 endA1 thi-1 hsdR17	Invitrogen

9. Plasmids

Plasmid	Description	Source or reference
pLV10	hc vector containing *nip1*Δ::*hisG*::*URA3*::*hisG* disruption cassette	L. Valasek
pRS315-*prt1-rnp1*-His	lc *LEU2* vector containing *prt1-rnp1*-His	Nielsen et al. 2006
pTZ - tif34Δ - URA	hc vector containing *tif34*Δ::*hisG*::*URA3*::*hisG* disruption cassette	K.Asano
pΔprt1#7	hc vector containing *prt1*Δ::*hisG*::*URA3*::*hisG* disruption cassette	K. Nielsen
pΔtif35#9	hc vector containing *tif35*Δ::*hisG*::*URA3*::*hisG* disruption cassette	K. Nielsen
YCp22-MET-NIP1-W	sc *TRP1* vector containing *NIP1* under *MET3* promotor	M. Karaskova
YCp22-MET-PRT1-W	sc *TRP1* vector containing *PRT1* under *MET3* promotor	A. Herrmannova
YCpprt1-1-His-U	lc *URA3* vector containing *prt1-1*-His	A. Hinnebusch
YEp112	hc *TRP1* vector	Gietz and Sugino 1988
YEp11-MET-TIF34-L	hc *LEU2* vector containing *TIF34* under *MET3* promotor	O. Janouskova
YEp11-MET-TIF35-L	hc *LEU2* vector containing *TIF35* under *MET3* promotor	O. Janouskova
YEpNIP1-His	hc *URA3* vector containing *NIP1-His*	Valasek et. al. 2002
YEpprt1-1-His-TIF34-TIF35-W	hc *TRP1* vector containing *prt1-1*-His, *TIF34* and *TIF35*	This study
YEpPRT1-His-TIF34-TIF35-W	hc *TRP1* vector containing *PRT1*-His, *TIF34* and *TIF35*	This study
YEpprt1-rnp1-His-TIF34-TIF35-W	hc *TRP1* vector containing *prt1-rnp1*-His, *TIF34* and *TIF35*	This study
YEpPRT1-TIF34-TIF35-U	hc *URA3* vector containing *PRT1*, *TIF34* and *TIF35*	L. Valasek
YEpPRT1-U	hc *URA3* vector containing *PRT1*	L. Valasek
YEpTIF32-NIP1-L	hc *LEU2* vector containing *TIF32* and *NIP1*	This study

YEpTIF32-nip1-Δ60-L	hc *LEU2* vector containing *TIF32* and *NIP1* truncated by 60 amino acid residues in its CTD	This study
YEptif32-Δ8-NIP1-His-L	hc LEU2 vector containing TIF32 with the deletion of first 200aa and NIP1-His	L. Valasek
YEptif32-Δ8-NIP1-L	hc *LEU2* vector containing *TIF32* truncated by 200 amino acid residues in its NTD and *NIP1*	This study
YEp-TIF34	hc *URA3* vector containing *TIF34*	Asano et al.1998
YEp-TIF35	hc *URA3* vector containing *TIF35*	Asano et al.1998

10. Oligonucleotides

Name	Sequence (5´to3´)
MJNIP1Sal-Xba	AGCAAAGAGTCAAGAAAGTTTCTA
NIP1-noHis-BamHI-R	TTATTGGATCCTCAACGACGATTTGATGGTGGGTTA AGACG
PBNIPD60-BamHI-R	CCCCGGATCCTCACACCTTATTTTCTGGAAGATC
PRT1-8xHis-F	ATTTCATGAACTTACGGGCTTGTATGTAAA
PRT1-8xHis-PstI-R	TTTACATACAAGCCCGTAAGTTCATGAAATCTGCAG TTAGTGGTGGTGGTGGTGGTGGTGTTCGACCTT TTCCTTTGTTTCTTCCAAAAC
PRT1-SpeI	GACGTGAAGACTAGTGTGTTC
PRT1-SphI-R	TGCGTCTACTTGTGCATGCAT

11. Cultivation media

11.1. Bacterial cultivation media and plates

LB medium: 10 g/L Bacto tryptone; 5 g/L Bacto yeast extract; 5 g/L NaCl (if needed add Ampicilin to final concentration 150 μg/mL).

LB/Amp plates: 10 g/L Bacto tryptone; 5 g/L Bacto yeast extract; 5 g/L NaCl; 25 g/L agar; Ampicilin to final concentration 50 mg/mL.

SOC medium: 20 g/L Bacto tryptone; 5 g/L Bacto yeast extract; 0.6 g/L NaCl; 0.2 g/L KCl; 3.5 g/L glucose.

11.2. Yeast cultivation media and plates

SC-LEU-TRP medium: 1.5 g/L SC-LEU-TRP (synthetic complete drop-out), 1.45 g/L YNB (yeast nitrogen base without AA and ammonium sulfate), 5 g/L ammonium sulfate, 20 g glucose

SC-LEU-TRP plates: 1.5 g/L SC-LEU-TRP (synthetic complete drop-out), 1.45 g/L YNB (yeast nitrogen base without AA and ammonium sulfate), 5 g/L ammonium sulfate, 20 g glucose, 25 g/L agar

SD medium: 1.45 g/L YNB (yeast nitrogen base without AA and ammonium sulfate), 5 g/L ammonium sulfate, 20 g glucose

SD plates: 1.45 g/L YNB (yeast nitrogen base without AA and ammonium sulfate), 5 g/L ammonium sulfate, 20 g glucose, 25 g/L agar

YPD medium: 20 g/L Bacto peptone, 10 g/L Bacto yeast extract, 20 g/L glucose

YPD plates: 20 g/L Bacto peptone, 10 g/L Bacto yeast extract, 20 g/L glucose, 25 g/L agar

5-FOA plates: 1.44 g/L YNB (yeast nitrogen base without AA and ammonium sulfate), 5 g/L ammonium sulfate, 20 g glucose, 25 g/L agar, 20 mM uracil, 1 g/L 5-FOA

12. Bacterial and yeast cultivation

12.1. Bacterial cultivation

Bacteria were grown in liquid media at 37°C while shaking or on agar plates at 37°C in an incubator.

12.2. Yeast cultivation

Yeast strains were grown in liquid media at 30°C while shaking or on agar plates at 30°C in an incubator. Temperature sensitivity and growing phenotype were tested at 34° and 37°C.

12.3. Permanent strain collections

Bacterial strains were stored on agar plates at 4°C for short terms and at -80°C in 40% glycerol for long terms. Yeast strains were stored on agar plates at 4°C for short terms and at -80°C in 20% glycerol for long terms.

12.4. Doubling time calculation

Doubling time was calculated for specific strains in this study according to the following formula: $[\ln(2)/\ln(OD_{END}/OD_{BEGIN})]$*time of growing

13. DNA manipulation

13.1. Plasmid DNA isolation – GenElute™ HP Plasmid Miniprep Kit (Sigma)

The miniprep procedure is based on alkaline lysis of bacterial cells followed by adsorption of DNA onto silica membrane in the presence of high salt. Bacteria are lysed under alkaline conditions, and the lysate is subsequently neutralized and adjusted to

high-salt binding conditions. DNA is adsorbed onto silica membrane while RNA, cellular proteins and metabolites are not retained on the membrane but are found in the flow-through.

Kit contains: Resuspension solution, RNase A solution, Lysis buffer, Neutralization/Binding buffer, Column preparation solution, Wash solution 1, Wash solution 2, Elution solution(10 mM Tris-HCl, pH=8.5), GenElute HP Miniprep binding columns, Collection tube (2 mL)

- Inoculate *E. coli* cells bearing plasmid of your interest into 2 mL of LB/Amp medium and grow them over night.
- Pellet the cells by centrifugation at 13000 rpm for 30 seconds.
- Resuspend the pellet in 200 μL Resuspension solution (containing RNase A) .
- Add 200 μL Lysis buffer and mix thoroughly by inverting the tube 4-6 times. Allow to clear, 3-5 minutes.
- Add 350 μL Neutralization/Binding buffer and mix immediately and thoroughly by inverting the tube 4-6 times.
- Centrifuge at 13000 rpm for 10 minutes.
- Insert Miniprep binding column into provided microcentrifuge tube. Add 500μL of Column preparation solution. Centrifuge at 13000 rpm for 1 minute. Discard flow-through liquid.
- Transfer the cleared lysate to the spin column and centrifuge at 13000 rpm for 30 seconds, discard the flow-through.
- Wash the spin column by adding 500 μL of Wash solution 1 and centrifuging at 13000 for 30 seconds. Discard the flow-through.
- Wash the spin column by adding 750 μL of Wash solution 2 and centrifuging at 13000 for 30 seconds. Discard the flow-through and spin for an additional 1 minute to remove residual wash buffer.
- Place the spin column in a clean microcentrifuge tube.
- To elute DNA add 100 μL water to the center of spin column, let stand for 1 minute and centrifuge at 13000 rpm for 1 minute, usual concentration of DNA isolated by this method is 0.2 μg/μL.

13.2. DNA modifications

Digestion by restriction endonucleases was done according to instructions provided by Roche and NEB companies and supplied reaction buffers were used.
For ligation reactions was used T4 DNA ligase (Roche) and supplied reaction buffer. T4 DNA ligase catalyzes the formation of phosphodiester bonds between neighbouring 3´-hydroxyl and 5´-phosphate ends in dsDNA. This enzyme will join blunt end and cohesive end termini as well as repair single stranded nicks in dsDNA.

13.3. Agarose gel electrophoresis

Agarose gel electrophoresis is a method used to separate DNA or RNA molecules by size. This is achieved by moving negatively charged nucleic acid molecules through an agarose matrix with an electric field. For estimating size and concentration of DNA on the gel was used 1 Kb Plus DNA Ladder (Invitrogen).

- Dissolve 1% of agarose in 1x TBE by heating in microwave oven.
- After cooling down to approximately 60°C add ethidium bromide to final concentration 0.5 μg/mL.
- Stir the solution to disperse the ethidium bromide, then pour it into the gel rack and insert the comb.
- When the gel has cooled down and become solid, remove the comb and put the gel with the rack into a tank with 1xTBE.
- Load the samples mixed with Sample buffer for agarose gel electrophoresis.
- Apply current, voltage 5 V/cm for approximately 1 hour.

13.4. Isolation of DNA from the gel - QIAEX®II Gel extraction Kit (Qiagen)

Extraction and purification of DNA fragments are based on solubilization of agarose and selective adsorption of DNA to the silica-gel particles in the presence of high salt. All impurities such as agarose, proteins, salts and ethidium bromide are

removed during washing steps. Elution of the DNA is accomplished with a low-salt solution such as water.

Kit contains: QIAEX II Suspension, Buffer QX1 and Buffer PE

- Excise the DNA band from agarose gel with a clean scalpel.
- Weigh the gel slice in a microcentrifuge tube and add 3 volumes of Buffer QX1 to 1 volume of gel.
- Add 15 μL QIAEX II Suspension to the sample and mix.
- Incubate at 50°C for 10 minutes, mix every 2 minutes to keep QIAEX II in suspension.
- Centrifuge at 13000 rpm for 30 seconds, remove supernatant.
- Wash the pellet with 500 μL of Buffer QX1.
- Wash the pellet twice with 500 μL of Buffer PE.
- Air-dry the pellet for 10 – 15 minutes until the pellet becomes white.
- To elute DNA add 20 μL of water, resuspend the pellet by vortexing and incubate in 50°C for 10 minutes. Repeat this step.
- Centrifuge at 13000 rpm for 30 seconds and save the supernatant.

13.5. Polymerase chain reaction (PCR)

Polymerase chain reaction was used to construct several recombinant vectors in this study. Typical PCR amplification program is shown in Table 1. Annealing temperature was adjusted according to the melting temperature of primers used in the reaction. Elongation time was adjusted according to the length of a fragment being amplified (1 minute/1kb length).

	Temperature	Time	
Initial denaturation	95°C	5 minutes	
Denaturation	95°C	1 minute	
Annealing	55°C	1 minute	25x
Elongation	72°C	1 minute	
Final elongation	72°C	5 minutes	
	4°C	hold	

Table 1. PCR amplification program

Composition of PCR reactions: 1x ThermoPol Reaction Buffer (NEB), 800 μM dNTP mix (200 μM of each), ~20 ng template DNA, 2 μM primers, 1 Unit VentR®DNA Polymerase (NEB), ddH_2O to a final volume of 50 μL.

13.6. Sequencing

All sequencing analysis was conducted at Centre Of DNA Sequencing at Institute of Microbiology, Academy of Science of Czech Republic. For sequencing reaction was used template DNA prepared by QIAprep Spin Miniprep Kit and specific primers in concentration 10 pmol/μL. The sequencing data were analyzed with BioEdit and Clone Manager programmes.

13.7. Introducing DNA into target cells

13.7.1. Transformation of *E. coli* by electroporation method

This method was used for introducing newly constructed vectors directly from the ligation reaction.

- Thaw electrocompetent cells (EP-MAX^{TM} 10B Competent Cells) on ice.
- Mix 20 μL of the cells and 1 μL of the ligation reaction in a clean microcentrifuge tube.
- Transfer the mixture into precooled electroporation cuvette (Eppendorf).

- Apply the pulse in the Gene Pulser Xcell Electroporation System using the „E. coli 1mm“ setting (conditions : 1,8 kV; 25 μF; 200 Ω).
- Immediately add 180 μL of SOC medium and transfer to a clean microcentrifuge tube.
- Incubate for 30 minutes at 37°C with shaking.
- Spread on LB/Amp plate.

13.7.2. Transformation of *E. coli* by heat-shock method

This method was used for introducing plasmid DNA isolated by GenEluteTM HP Plasmid Miniprep Kit (Sigma).

- Thaw competent cells (Subcloning Efficiency^{TM} DH5α^{TM} Competent Cells) on ice.
- Mix 200 μL of the cells with 1 μL of plasmid DNA (500 ng) and incubate on ice for 30 minutes.
- Heat shock cells at 42°C for 40 seconds.
- Add 400 μL of SOC medium and incubate for 30 minutes at 37°C with shaking.
- Spread on LB/Amp plate.
-

13.7.3. Transformation of *S. cerevisiae* by LiAc transformation method

- Grow the *S. cerevisiae* strain you want to transform in 50 mL of liquid media (SD or YPD) to OD_{600} of approximately 0.5.
- Centrifuge at 2500 rpm for 3 minutes and discard supernatant. Wash the cells in 5 mL 1xLiAc/TE.
- Resuspend the cells in 200 μL 1x LiAc/TE. Add 20 μL of Salmon sperm DNA (Invitrogen)
- Mix 50 μL of the cells with 1 μL of plasmid DNA (500 ng) and 300 μL PEG/LiAc/TE solution.
- Incubate at 30°C for 30 minutes with shaking.
- Incubate at 42°C for 15 minutes without shaking.
- Add 1 mL dH_2O and centrifuge at 2500 rpm for 3 minutes, discard supernatant.

- Add 200 µL dH_2O and spread on appropriate plate.

14. Protein manipulation

14.1. WCE preparation for analysis by Western blotting

- Grow yeast cell culture in 100 mL of liquid media to OD_{600} of 1.
- Centrifuge at 4000 rpm for 5 minutes at 4°C, discard supernatant.
- Wash with 10 mL of ice cold dH_2O.
- Resuspend the cells in 1 mL per gram (wet weight) of cells in BB buffer and add 4 mm diameter acid-washed glass beads equal to one half of the total volume of resuspended cells. Hold your samples on ice.
- Vortex for 30 seconds followed by 1 minute on ice, repeat 8 times.
- Centrifuge at 3000 rpm for 5 minutes at 4°C.
- Transfer supernatant into precooled microcentrifuge tube and centrifuge at 13000 rpm for 10 minutes at 4°C.
- Carefully transfer supernatant into new precooled microcentrifuge tube.
- Save the supernatant.

14.2. SDS-PAGE

- Mix samples for SDS-PAGE with 4x sample loading buffer and boil for 5 minutes at 95°C.
- Put Criterion Precast Gel into electrophoretic tank and pour in SDS-PAGE running buffer.
- Load samples on Criterion Precast Gel.
- Load Precision Plus Protein™ Standarts Dual Color (Bio-Rad).
- Apply current, voltage 200 V for 1 hour.

14.3. Western Blotting

- After SDS-PAGE assemble the blotting device (cathode, plastic net, sponge, filter paper, gel, nitrocellulose membrane, filter paper, 2 sponges, plastic net, anode)
- Fill the blotting tank with cool blotting buffer.
- Apply current, voltage 25 V for 1.5 hour.
- Reassemble the blotting device.
- Incubate the membrane in blocking solution (5% milk in TBS-T) for 1 hour.
- Cut the membrane apart if probing for different antibodies.
- Incubate every part of membrane with appropriate primary antibody diluted in blocking solution over night at 4°C.
- Wash the membrane strips with TBS-T three times for 10 minutes.
- Incubate the membrane strips with secondary antibody diluted in TBS-T for 1 hour at room temperature.
- Wash the membrane strips with TBS-T three times for 10 minutes.

14.4. Chemiluminiscent detection

- Assemble the membrane strips.
- Incubate with SuperSignal West Femto Maximum Sensitivity Luminol and SuperSignal West Femto Maximum Sensitivity Stable Peroxidase Buffer (1:1 solution) for 1 minute.
- Collect gradually increasing exposures at the G:BOX iChemi devise.

14.5. Gel blue staining

- After running SDS-PAGE wash the gel 5 minutes in water.
- Incubate 1 hour with Gel Code® Blue Stain Reagent.
- Destain 1 hour in water.

15. Purification of His-tagged eIF3 from *S. cerevisiae* (modified Acker et al. 2007)

15.1. Cultivation and concentrating for eIF3 purification

- From a glycerol stock, streak a sample of eIF3 yeast cells on a SC-LEU-TRP plate and grow at 30 ºC for 2 days.
- Take some yeast cells from plate inoculate in 5 mL SC-LEU-TRP media at 30 ºC O/N. Then transfer culture into 50-200 mL SC-LEU-TRP at 30 ºC O/N. Inoculate twelve 1.5 L cultures of SC-LEU-TRP media in 2800 mL baffled flasks with 10 mL of a 50-200 mL overnight starter culture per flask and grow over night at 30 ºC with shaking at 250 rpm.
- Concentrate the cultures up to the volume 500 mL using the Concentrator protocol (see chapter 15.4.).
- Spin down cells in a Beckman SX 4750A rotor at 4,000 rpm for 30 minutes at 4 ºC; discard media; dissolve all yeast pellets with a small volume of water and transfer to an empty bottle. Pellet cells again; weigh the yeast pellets.
- Dissolve cell pellets into smooth slurry using 1/3 volume of lysis buffer (low imidazole buffer, i.e. 30 g cells/10 mL buffer). Using a 10 mL pipette, drip the slurry into an ice bucket of liquid N_2. Collect frozen droplets into a plastic beaker; cover with aluminum foil and store at -80 ºC. The frozen yeast can be stored at -80 ºC for years.

15.2. Grinding frozen yeast droplets using FreezerMill 6870

- Fill container with liquid N_2. Cool down grinding vial in dry ice at least for 15 minutes.
- Fill 1/3 of the grinding vial with your frozen droplets, do not overfill the vial, and put it into FreezerMill 6870. Use the grinding protocol with 10 cycles, where one cycle consists of 5 minutes pre-cooling step, 1 minute of processing and 2 minutes of cooling down.
- Take out the vial. Remove one end plug using vial opener (slowly and in steps to avoid popping open). Pool powder into a plastic beaker and store at -80 ºC for next day prep. The yeast powder can be stored at -80 ºC for years.

- Use wipes to clean the edge of cylinder and plugs and repeat adding frozen cell drops for breaking cells.

15.3. Sample preparation and column loading

-Take out ~400 mL low imidazole buffer; add 8 tablets of Complete EDTA-free inhibitors (Roche, 50X), pepstatin A 1µg/mL (400µl, 1000X), aprotinin 1µl/mL (400µl, 1000X), benzamidine 1mM (400µl, 1000X), leupeptin 1µg/mL (400µl, 1000X) and DNase (100µl, Roche) to the powdered lysate. Stir until all powder is dissolved in cold room.

- Clarify the lysate by centrifugation in a Sorvall SS-34 rotor at 11,000 rpm for 30 minutes at 4 ºC. During this spin time, set up 5 mL HiTrap HP column (GE Healthcare) and equilibrate on an FPLC (low salt 0%/ high salt100%/low salt 0%). (UV detector should get flat line, maybe a small peak appears during buffer switch; avoid bubbles; buffers prepared one day before, filtered and cool down).

- Pool the supernatant (discard the last turbulent part); filter through 2 layers of 5 µm filter papers; pool the supernatant filter through 2 layers of 5 µm filter papers again, and 0.8 µm filter unit. Keep supernatant cool.

- Load the lysate onto the HiTrap HP column (GE Healthcare) at a flow rate of 3-5 mL/min. Wash the nickel column with low imidazole buffer 100 mL; collect 5 mL fractions, and elute with high imidazole buffer (nickel column elution buffer) at 5 mL/min; collect 1 mL fractions.

- Pool the appropriate fractions (the entire elution peak) (~15-20 mL) and concentrate to less than 1.5 mL using an Amicon Ultra concentrator (Millipore, 10K MWCO).

- Apply the half of 1.5 mL sample (using a 1 mL loop) to an 120 mL Superose 12 gel filtration column equilibrated in low salt buffer and elute with low salt buffer (flow rate of 0.5 mL/min; 1 mL/fraction collection). After ~100 mL elution, apply the rest of your sample for elution. Analyze fractions by SDS-PAGE using 10% polyacrylamide; 15 µl per fraction for loading; 200V ~50 min.

- Pool the appropriate fractions ~14 mL and load onto a freshly prepared 10 mL phosphocellulose column, which is equilibrated in low salt buffer. All the time take 5 mL fraction for collection.

- Wash the phosphocellulose column with ~50 mL of low salt buffer, than change into 20 mL B-200. Elute with 20 mL B-350. Wash the column with 20 m1 B-1000. Analyze by 10% SDS-PAGE gel as above. Pool the appropriate fractions (those enriched in stoichiometric eIF3) and dialyze into 2 L enzyme storage buffer over night.
- Concentrate and determine the protein concentration (the molecular mass of eIF3 is 361.3 kDa), flash-freeze in liquid N_2 and store at –80 ºC.

15.4. Concentrator protocol

The Pellicon 2 filtration system (Millipore) using the high-performance tangential flow filter Pellicon 2 cassette (0.45 μm) is the most efficient way to concentrate such a huge amount of yeast culture. The culture with the help of the peristaltic pump Easy-Load® Peristaltic Pump (Millipore) washes the filter and the flow-through (media without cells) is led into the sink, thus the culture is concentrated.

- Begin by setting up according to the official manual for Pellicon® 2 cassette (0.45μm) and Pellicon Cassette Acrylic Holder (Millipore). Join Easy-Load® Peristaltic Pump (Millipore).
- Pump ~ 5 L of dH_2O through making sure that liquid is clear and near neutral pH upon leaving cassette
- Place feed and retentate line into carboy containing broth, tape in place.
- Set rate to 50-60 and start the pump. Open the permeate valve to the first notch. Set the pressure on the feed side to 10 by clamping down on the retentate line. Maintain pressure at 10 for the duration of run.
- When volume gets very low (less than 500 mL) rinse with ~ 1 L cold ddH_2O. Allow volume to get low again, close permeate valve, open clam and pump remaining solution into centrifuge bottle to collect cells. Pump at a slower speed to avoid spillage.
- Add more ddH_2O to rinse the rest of cells through the cassette into centrifuge bottle.

- To wash the concentrator, pump ~10 L dH_2O through the cassette at rate 60. All valves open, both permeate and retentive lines in sink.
- Make 2 L of 0.5 M NaOH.

- Tape all lines into cylinder and let circulate 2 L of fresh 0.5 M NaOH at 50 for about 5-10 minutes.

15.5. Fresh phosphocellulose column preparation (~10 mL)

- Add 125 mL 0.5 M NaOH to ~0.8 g phosphocellulose (Whatman Co.). **S**tir for at least 5 minutes and gravity settle down. Discard supernatant.

- Wash matrix with ddH_2O (phosphocellulose will turn to white color) five times until its pH<11, detect it by pH paper .

- Add 125 mL 0.5 M HCl. Stir for at least 5 minutes and gravity settle down. Discard supernatant. Rinse with ddH_2O five times until its pH>4.

- Place in a gravity flow column for package. Wash the column with low salt buffer for equilibration three times until its pH~7.

- Resuspend matrix in the column; tighten and seal the column; place in cold room for package over night.

15.6. Stripping HiTrap HP column

- Use the 50 mL syringe and wash the column 5mL HiTrap HP column with 50 mL 100 mM EDTA in ddH2O
- Wash the column with 50 mL ddH2O
- Wash the column with 30 mL 100 mM NiSO4
- Wash the column with 50 mL ddH2O

Now the column is prepared for next usage.

15.7. Bradford assay – protein quantitation

The Bradford Reagent (SIGMA) can be used to determine the concentration of proteins in solution. The procedure is based on the formation of a complex between the dye, Brilliant Blue G, and proteins in solution (Bradford, 1976). The protein-dye complex causes a shift in the absorption maximum of the dye from 465 to 595 nm. The amount of absorption is proportional to the protein present.

- The standard curve for protein concentration measurement was established using BSA (NEB) in 1mL of Bradford reagent, the final concentration 1, 2, 4, 6, 9 and 10 μg/mL, where the absorbance is in the linear range.
- 1 μl of my protein was added into 1 mL of the dye and after 5 min it was measured its absorbance at 595 nm.
- The protein concentration was recalculated and the molarity was calculated with the molecular mass of the wild type eIF3 complex (361.3 kDa).

15.8. Nuclease contamination control

- Use the highest concentration of your protein sample, mix it with radiolabled mRNA (*RPL41A*) to final concentration 50 nM or 15 nM of mRNA depending on isotope activity and incubate it for 2 h at 30°C. As control use RNA without your protein.
- Use the RNA loading dye 2x (Fermentas), boil it for 1 min at 99°C.
- Load the samples onto a denaturating 4% acrylamide gel.
- To prepare 10 mL of denaturating 4% acrylamide gel use

1 mL	40% Acrylamide:Bis-Acrylamide (19:1)
9 mL	1x TBE with 8M urea
150 μL	10% APS
10 μL	10% TEMED

- Run the gel at 200 V for 50 min and subject the gel to autoradiography.

16. 43S gel shift assay (modified Acker et al. 2007)

43S gel shift assay is a powerful tool, how to monitor the binding of ternary complex and other factors to 40S subunits to form so called 43S complex. These stages can be separated with the native gel electrophoresis and visualized with radiolabled tRNA.

16.1. Acrylamide gel for the 43S gel shift assay

- Use 30x16 cm plates (one notched) and 0.45 mm spacers. Wash everything carefully. The gel is thin and soft. To help him to stick to the unnotched plate, scrub the plate with

steel wool during washing using water, soap, water, ethanol, water and again ethanol. Wash the notched plate with water, soap, water, and ethanol and never scrub this plate. Siliconize the surface of the notched plate with Sigmacote (Sigma). Clean 2.5 cm strip on the top, where the wells will be, with ethanol.

- Put both plates with spacers together and tape the sides and the bottom with the tape and use 6 clamps to hold it together.
- Insert the comb before pouring the gel pushing it about three quarter of the way in.

-Prepare 40 mL of 4% native gel

32 mL	ddH2O
4 mL	10x THEM
4 mL	40% Acrylamide:Bis-Acrylamide (37.5:1)
400 μL	10% APS
40 μL	10% TEMED

Mix it and pour the gel while the plates are horizontally.

- Before loading your sample remove the tape from plates and put it to the gel box (well behind gel- 26.5 cm wide, 19 cm tall, 2.5 cm deep; well in front of gel – 31 cm wide, 5.5 cm tall, 6.5 cm deep). Insert a coil of tubing, attached to a circulating water bath, into the gel box behind the gel. Make sure the coil doesn´t touch the gel plate. Fill the boxes with 1x THEM, remove bubbles. Start cooling at 16℃.
- Remove the comb and use the syringe to rinse out each well.
- Load your samples, run 2000 V; 25 W for 45 minutes
- Open the plates carefully and add the whatman paper to the gel. Gel sticks to the paper and can be removed from the plate.
- Expose your gel to an imaging plate BAS cassette 2025 (FUJIFILM) over night and scan your result with Molecular Imager FX™ (Bio-Rad).

16.2. 43S gel shift reaction

The final concentration of components in reaction:

1 μM eIF1

1 μM eIF1A

1 μM mRNA75.1

30 nM 40S ribosomal subunit

1 mM GDPNP

0.5 μM eIF2

1 nM radiolabled tRNA

1xRecon buffer

various eIF3

- Prepare the 20μl reactions with various concentrations of eIF3.
- To establish the ternary complex (TC), pre-incubate GDPNP and eIF2 for 10 minutes at 26℃ in water bath, add the radiolabled tRNA and incubate additional 5 minutes at 26℃.
- Add the TC to the rest of the components and incubate the reactions 30 minutes at 26℃.
- After the incubation add the native gel dye and load your samples on the 4% native gel.

17. mRNA recruitment assay

mRNA recruitment assay can monitor the speed of the mRNA binding to certain complex based on its gel shift in time.

17.1. Acrylamide gel for the mRNA recruitment assay

- Use two 9x14cm plates. One notched (ceramic) and the second unnotched (glass). Wash both plates carefully with soap, water and ethanol.
- Prepare 10 mL of 4% native gel

8 mL	ddH2O
1 mL	10x THEM
1 mL	40% Acrylamide:Bis-Acrylamide (37.5:1)
150 μL	10% APS
10 μL	10% TEMED

Mix it and pour the gel.

- Before loading place your gel into an electrophoretic box. Fill the box with 1x THEM. Start cooling at 22℃.

- Remove the comb and use the syringe to rinse out each well.
- Load your samples while running at 75 V, than change and run the gel at 200 V for 50 minutes
- Open the plates carefully and add the Whatman paper to the gel. Gel sticks to the paper and can be removed from the plate.
- Expose your gel to an imaging plate BAS cassette 2025 (FUJIFILM) for 30 minutes and scan your result with Molecular Imager FX™ (Bio-Rad).

17.2. mRNA recruitment reaction

The final concentration of components in reaction:

1 μM eIF1
1 μM eIF1A
1 μM eIF4A
1 μM eIF4B
50 nM eIF4E/G
30 nM 40S ribosomal subunit
2 mM ATP
1 mM GDPNP
0.2 μM eIF2
0.2 μM Met-tRNA$_i^{Met}$
0.2 μM or 0.4μM eIF3
15 nM radiolabeled mRNA *RPL41A*
1x Recon buffer

- Prepare the 10 μl reaction for each time point.
- To establish the ternary complex (TC), pre-incubate GDPNP and eIF2 for 10 minutes at 26°C in water bath, add the tRNA and incubate additional 5 minutes at 26°C.
- Add the TC to the rest of the components except the mRNA and incubate the reactions 120 minutes at 26°C.
- At specified time points add the radiolabeled mRNA.
- To stop the reaction add the native gel dye and immediately load your samples on the running 4% native gel.

17.3. Hot capping of mRNA *RPL41A*

For the mRNA recruitment assay the radioactively labeled capped mRNA is needed.

The final concentration of components in reaction:

1x enzyme storage buffer

1 mM GTP

2 μCi/μL [α^{32}P]GTP

100 μM SAM

1 U/μL RNase inhibitor

5 μM mRNA

125 nM vaccinia capping enzyme (NEB)

- Mix the 50 μL reaction without the enzyme and incubate the mixture at 37°C for 30 minutes.
- Add the vaccinia capping enzyme and incubate at 37°C for additional 30 minutes.
- Purify the mRNA using the RNeasy Mini Kit (Qiagen).
- Measure the absorbance of the mRNA, for the concentration calculation use the extinction coefficient for *RPL41A* (2257220 M^{-1}. cm^{-1})
- For the next and better use dilute part of your sample to the concentration of 150 nM.

Results

18. Preparation of mutant eIF3 complexes for its testing in *in vitro* assays

To address the major aim of my thesis; i.e. to identify specific domains of eIF3 that promote mRNA recruitment with help of *in vitro* reconstituted system of translation initiation, I first had to search the currently available literature to carefully select all specific eIF3 mutations displaying phenotypes indicative of the mRNA recruitment defect. In the first round of analysis described herein the following three mutations were picked: *prt1-1*, *prt1-rnp1*, *nip1-Δ60*; the description of their *in vivo* effects can be found in section Review of previous research (chapter 13.). Subsequently, I had to prepare strains overexpressing all five eIF3 subunits with the PRT1 subunit carrying a C-terminal His tag, where only a chosen mutant allele of a given eIF3 subunit is produced in place of its corresponding wt gene. Finally, I had to purify the mutant eIF3 complexes to examine their effects on the selected initiation reactions described below.

18.1. Construction of recombinant vectors used for overexpression of all five eIF3 subunits

Purification of mutant eIF3 complexes was planned using the Ni2+ chelation chromatography, and placing the 8xHis tag at the C-terminus of PRT1 turned out to be, based on our previous tests, the most effective way of pulling down sufficient amounts of eIF3 from cells. To insert the 8xHis tag into the overexpresing vector YEpPRT1-TIF34-TIF35-U, the fusion PCR was performed using the following pairs of primers PRT1-SpeI – PRT1-8xHis-PstI-R and PRT1-8xHis-F – PRT1-SphI-R, with YEpPRT1-TIF34-TIF35-U as a template. The PCR products thus obtained were used in a 1:1 ratio as templates for a third PCR amplification with primers PRT1-SpeI and PRT1-SphI-R. The resulting PCR product was digested with *Spe*I-*Sph*I and inserted into *Spe*I-*Sph*I-digested YEpPRT1-TIF34-TIF35-U producing YEpPRT1-His-TIF34-TIF35-U.

To produce YEpPRT1-His-TIF34-TIF35-W, *URA3* was replaced by *TRP1* by cutting YEpPRT1-His-TIF34-TIF35-U with *Ahd*I-*Sac*I and replacing the ~4-kb fragment with the ~3.7-kb long *Ahd*I-*Sac*I-digested fragment from YEp112.

YEpTIF32-NIP1-L was generated by PCR using primers MJRNIP1Sal-Xba and NIP1-noHis-BamHI-R, and YEpTIF32-NIP1-His-L as a template. The resulting PCR product was digested with *Xba*I-*Bam*HI and inserted into *Xba*I-*Bam*HI cleaved YEpTIF32-NIP1-His-L to produce YEpTIF32-NIP1-L.

YEpTIF32-nip1-Δ60-L was generated by PCR using primers MJRNIP1Sal-Xba and PBNIPD60-BamHI-R, and YEpTIF32-NIP1-L as a template. The resulting PCR product was digested with *Xba*I-*Bam*HI and inserted into *Xba*I-*Bam*HI cleaved YEpTIF32-NIP1-L.

YEpprt1-1-His-TIF34-TIF35-W was generated by PCR using primers PRT1-SpeI and PRT1-8xHis-PstI-R, and YCpprt1-1-His-U as a template. The resulting PCR product was digested with *Spe*I-*Pst*I and inserted into *Spe*I-*Pst*I cleaved YEpPRT1-His-TIF34-TIF35-W.

To produce YEpprt1-rnp1-His-TIF34-TIF35-W, ~2.3-kb fragment digested from pRS315-*prt1-rnp1*-His with *Spe*I-*Ahd*I was inserted into *Spe*I-*Ahd*I cleaved YEpPRT1-His-TIF34-TIF35-W.

To produce YEptif32-Δ8-NIP1-L, ~3.2-kb fragment digested from YEptif32-Δ8-NIP1-His-L with *Msc*I-*Pst*I was inserted into *Msc*I-*Pst*I cleaved YEpTIF32-NIP1-L.

18.2. Preparation of yeast strains

The yeast haploid strain H505 (*prb1Δ pap4Δ*) with the double deletion of peptidases PRB1 and PAP4 showed the highest yield of purified wt eIF3. For the purpose of this study the best option was to introduce a single deletion of a chromosomal allele of each eIF3 subunit into this strain at a time, so that mutant eIF3 complexes carrying mutations in a given eIF3 subunit could be isolated for follow up experiments. In other words, I created five H505 (*prb1Δ pap4Δ*) derivatives - each containing a single deletion of a different eIF3 subunit, which expressed a wt allele of the deleted subunit on a shuffling plasmid instead. In the next step these wt alleles were individually replaced by selected plasmid-borne mutants by plasmid shuffling. Thus all eIF3 complexes

purified from thus generated mutant strains by affinity chromatography contained only the mutant protein of a given subunit and not a mixture of wt and mutant proteins.

To create PBH57 (*prb1Δ pap4Δ tif34Δ* YEp-TIF34) and PBH42 (*prb1Δ pap4Δ tif35Δ* YEp-TIF35), *LEU2*–based covering plasmids YEp11-MET-TIF34-L and YEp11-MET-TIF35-L, expressing TIF34 and TIF35 under the control of the methionine promoter, respectively, were first introduced into the H505 (*prb1Δ pap4Δ*) strain using the LiAc yeast transformation protocol. The resulting transformants were first selected on SD media lacking leucine and methionine. Positively scoring clones were subsequently transformed with the *tif34Δ::hisG::URA3::hisG* (pTZ-tif34Δ-URA) and *tif35Δ::hisG::URA3::hisG* (pΔtif35#9) disruption cassettes, respectively, to delete a gene of a given eIF3 subunit. The URA+ colonies were selected on SD-URA plates and the uracil auxothrophy was subsequently regained by growing the transformants on 5-FOA containing plates. Successful completion of these genetic manipulations was verified by growing the resulting strains, auxotrophic for uracil, on plates supplemented with or lacking methionine. Only those cells, where a chromosomal allele of a given eIF3 subunit was completely deleted, failed to grow on media containing methionine. Thus generated and verified strains were finally transformed with YEp-TIF34 and YEp-TIF35 and the leucine auxotrophy (a loss of the original covering plasmids YEp11-MET-TIF34-L and YEp11-MET-TIF35-L, respectively) was regained by growing the cells in liquid media containing leucine for several rounds of exponential growth and selecting for those clones that did grow in the absence of uracil but not in the absence of leucine in the media. The resulting strains were named PBH57 (*prb1Δ pap4Δ tif34Δ* YEp-TIF34) and PBH42 (*prb1Δ pap4Δ tif35Δ* YEp-TIF35).

To create PBH44 (*prb1Δ pap4Δ prt1Δ* YEpPRT1-U) and PBH56 (*prb1Δ pap4Δ nip1Δ* YEpNIP1-His), *TRP1*–based covering plasmids YCp22-MET-PRT1-W and YCp22-MET-NIP1-W, expressing PRT1 and NIP1 under the control of the methionine promoter, respectively, were first introduced into the H505 (*prb1Δ pap4Δ*) strain using the LiAc yeast transformation protocol. The resulting transformants were first selected on SD media lacking tryptophan and methionine. Positively scoring clones were subsequently transformed with the *prt1Δ::hisG::URA3::hisG* (pΔprt1#7) and *nip1Δ::hisG::URA3::hisG* (pLV10) disruption cassettes, respectively, to delete a gene of

a given eIF3 subunit. The URA+ colonies were selected on SD-URA plates and the uracil auxothrophy was subsequently regained by growing the transformants on 5-FOA containing plates. Successful completion of these genetic manipulations was verified by growing the resulting strains, auxotrophic for uracil, on plates supplemented with or lacking methionine. Only those cells where a chromosomal allele of a given eIF3 subunit was completely deleted failed to grow on media containing methionine. Thus generated and verified strains were finally transformed with YEpPRT1-U and YEpNIP1-His and the tryptophan auxotrophy (a loss of the original covering plasmids YCp22-MET-PRT1-W and YCp22-MET-NIP1-W, respectively) was regained by growing the cells in liquid media containing tryptophan for several rounds of exponential growth and selecting for those clones that did grow in the absence of uracil but not in the absence of tryptophan in the media. The resulting strains were named PBH44 (*prb1Δ pap4Δ prt1Δ* YEpPRT1-U) and PBH56 (*prb1Δ pap4Δ nip1Δ* YEpNIP1-His).

To produce PBH64 (*prb1Δ pap4Δ nip1Δ* YEpPRT1-His-TIF34-TIF35-W YEpTIF32-NIP1-L) and PBH65 (*prb1Δ pap4Δ nip1Δ* YEpPRT1-His-TIF34-TIF35-W YEpTIF32-nip1-Δ60-L) overexpressing all eIF3 subunits, PBH56 (*prb1Δ pap4Δ nip1Δ* YEpNIP1-His) was first subjected to double transformation with YEpPRT1-His-TIF34-TIF35-W and YEpTIF32-NIP1-L or with YEpPRT1-His-TIF34-TIF35-W/YEpTIF32-nip1-Δ60-L, respectively. The resulting double transformants were selected on SD-LEU-TRP but +URA to minimize the number of revertants generated during this procedure for unknown reasons. The resident *URA3*-based YEpNIP1-His plasmid carrying was contra-selected against on SD plates containing 5-FOA.

To produce PBH52 (*prb1Δ pap4Δ prt1Δ* YEpPRT1-His-TIF34-TIF35-W YEpTIF32-NIP1-L), PBH54 (*prb1Δ pap4Δ prt1Δ* YEpprt1-rnp1-His-TIF34-TIF35-W YEpTIF32-NIP1-L) and PBH55 (*prb1Δ pap4Δ prt1Δ* YEpprt1-1-His-TIF34-TIF35-W YEpTIF32-NIP1-L) overexpressing all eIF3 subunits, PBH44 (*prb1Δ pap4Δ prt1Δ* YEpPRT1-U) was first subjected to double transformation with YEpPRT1-His-TIF34-TIF35-W and YEpTIF32-NIP1-L, YEpprt1-rnp1-His-TIF34-TIF35-W/YEpTIF32-NIP1-L or with YEpprt1-1-His-TIF34-TIF35-W / YEpTIF32-NIP1-L, respectively. The resulting double transformants were selected on SD-LEU-TRP but +URA to minimize

the number of revertants. The resident *URA3*-based YEpPRT1-U plasmid carrying was contra-selected against on SD plates containing 5-FOA.

To produce PBH50 (*prb1Δ pap4Δ tif32Δ* YEpPRT1-His-TIF34-TIF35-W YEpTIF32-NIP1-L) and PBH51 (*prb1Δ pap4Δ tif32Δ* YEpPRT1-His-TIF34-TIF35-W YEptif32-Δ8-NIP1-L) overexpressing all eIF3 subunits, H507 (*prb1Δ pap4Δ tif32Δ* YCpTIF32-His-U) was first subjected to double transformation with YEpPRT1-His-TIF34-TIF35-W and YEpTIF32-NIP1-L or with YEpPRT1-His-TIF34-TIF35-W/ YEptif32-Δ8-NIP1-L, respectively. The resulting double transformants were selected on SD-LEU-TRP but +URA to minimize the number of revertants. The resident *URA3*-based YCpTIF32-His-U plasmid carrying was contra-selected against on SD plates containing 5-FOA.

18.3. Phenotypical control

Before proceeding to the purification steps, it was necessary to check the phenotype of the newly generated, mutations-carrying strains in order to confirm their known *in vivo* effects on the cell growth. This double-checking was desirable to make sure that our mutants in the genetic background of H505 (*prb1Δ pap4Δ*) will show the same phenotypes as they did in their original genetic background. Where possible (in case of larger truncations or internal deletions), a presence of the only mutant allele of a given eIF3 subunit in the mutant strains was also verified by Western blotting.

The grow defects, slow growth (Slg-) and temperature sensitivity (Ts-) were monitored with help of a classical colony spot assay, where the cells were spotted in serial 10-fold dilutions onto SD plates supplemented with required nutrients and incubated at 30°, 34° and 37°C.

eIF3 subunit	Mutation	Phenotype	Reference
TIF32	*tif32-Δ8*	Slg-; severe Gcn-	Szamecz et al. 2008
PRT1	*prt1-1*	Slg-; severe Ts-	Nielsen et al. 2004
	rnp1	Slg-; severe Ts-	Nielsen et al. 2006
NIP1	*nip1-Δ60*	Slg-; Gcn-	Kouba et al. 2011
TIF34	*tif34-DDKK*	severe Ts-	Herrmannova et al. 2011

Table 2. Representative example of the eIF3 mutants tested in this study

As shown in Fig. 6, the detected phenotypes of all tested strains nicely correspond to the phenotypes of the original mutant strains as published by (Herrmannová et al., 2011; Kouba et al., 2011; Nielsen et al., 2004, 2006; Szamecz et al., 2008) (see Table 2 summarizing the originally reported *in vivo* effects).

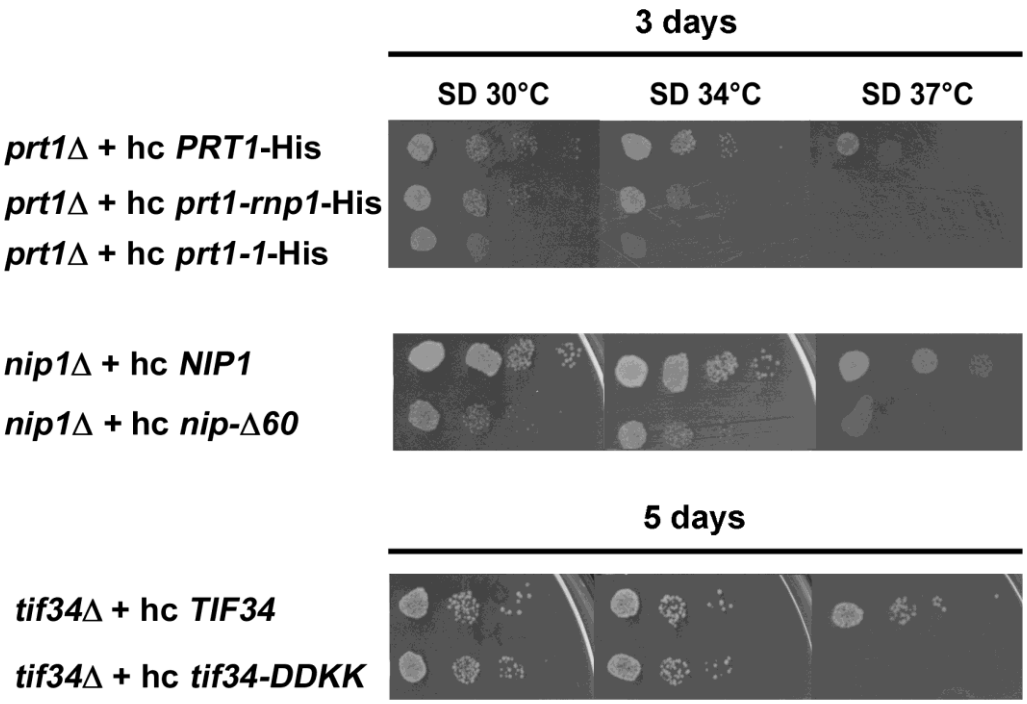

Figure 6. The growth phenotypes of the selected yeast strains. Indicated strains were spotted in four serial 10-fold dilutions on SD plates supplemented with required nutrients and incubated at 30°C, 34°C, or 37°C for 3 or 5 days, respectively.

The *tif32-Δ8* truncation is one of those mutations that can be detected by Western blotting (see chapter 14.). It removes the first 200 amino acid residues of the TIF32 subunit of eIF3. Hence both newly made strains in PBH50 and PHB51 were analyzed by Western blotting using the monoclonal anti-TIF32 antibody. As shown in Fig. 7, whereas PBH50 expresses only the wt full-length TIF32 protein running at ~130 kDa position, PBH51 carries the truncated (*Δ8*) version of TIF32 running at 110 kDa but not the wt protein.

All mutant strains that passed all verification tests were then ready for subsequent purification steps. In the reminder of my work I mention only those strains/eIF3 mutants, the biophysical analysis of which has been completed by the time of completion of my Diploma work.

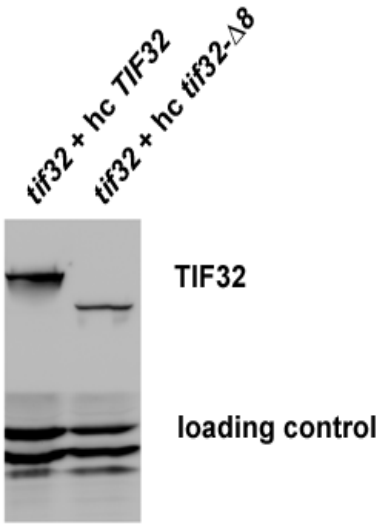

Figure 7. Western blot detection of a truncated form of TIF32 in *tif32-Δ8* expressed by the PBH51 strain. TIF32 proteins were detected by the monoantibodies directed against TIF32 (Jirincová et al., 1998); the loading control mixture of proteins was visualized with the mixture of antibodies against TIF34, TIF35, and RPS0A.

19. Purification protocol of mutant eIF3 complexes

Mutant eIF3 complexes were purified from the corresponding overexpressing strains by a well established protocol that is described in detail in chapter 15. in Material and methods. In some cases it was necessary to modify this protocol according to the specific properties of given mutant complexes. The main changes are described further in the text.

19.1. Yeast cell lysate preparation

First, the doubling time was measured for the following strains PBH54, PBH55 and PBH65 grown in SC media lacking leucine and tryptophane (Table 3)(see chapter 12.4.). Strains PBH54, PBH55 and PBH65 are producing mutant eIF3 complexes eIF3-rnp1, eIF3-prt1-1 and eIF3-Δ60; please note that the latter designation is used throughout the rest of this study.

Strain	Doubling time
PBH54 (eIF3-rnp1)	3 h
PBH55 (eIF3-prt1-1)	5,3 h
PBH65 (eIF3-Δ60)	2,5 h

Table 3. Doubling time of selected yeast strains.

Overnight inoculum of each strain was prepared, diluted in 9L of fresh SC-LEU-TRP media and grown while shaking to an OD_{600} of around 7. I decided to use only 9 liter culture instead of 18 liters to minimize the risk of contaminating my slowly growing cultures. Ultimately it had no effect on the experiment as the wet volume obtained from 9 liters turned out to be sufficient for getting enough of the purified complexes. The harvested cultures were firstly concentrated on the cell concentrator to reduce the volume to around 0.5 L and then spun down in a large capacity centrifuge (Beckman SX 4750A). The resulting yeast pellets were weighed and suspended into a smooth slurry using 1mL of low imidazole buffer (see chapter 6.) per 3g of yeast pellets. Each slurry was then slowly dropped into liquid nitrogen and the frozen droplets were collected and stored at -80C. Frozen cells were lysed using the Freezer mill 6870; a frozen powder of a cell lysate was produced and processed further as described below.

19.2. Purification of mutant eIF3 complexes from the cell lysate

Each cell lysate was dissolved in 150 mL of low imidazole buffer (see chapter 6.) supplemented with a fresh cocktail of protease inhibitors. The lysate was then clarified by centrifugation and the supernatant was filtered through 2 layers of 5 µm filter papers using a 0.8 µm filter unit, before it was loaded onto an equilibrated nickel column connected to the FPLC (Äcta, GE Healthcare). The loading, washing and elution steps using the HiTrap HP column were carried out according to the vendor (GE Healthcare). All fractions corresponding to the entire elution peak were pooled together (fractions 15-30 for eIF3-rnp1; 35-54 for eIF3-prt1-1; and 12-20 for eIF3-Δ60) and concentrated using an Amicon Ultra concentrator (Millipore, 10K MWCO) to the final volume smaller than 2 mL.

The concentrated sample was divided into two parts and applied to a 120 mL Superose 12 gel filtration column (GE Healthcare) to get a better resolution between the elution peak and the shoulder, which usually consist of partial subcomplexes. Ultimately, the purified complexes were eluted in a low salt buffer (see chapter 6.). Fractions from the top of individual elution peaks were analyzed by SDS-PAGE, followed by gel blue staining (see chapter 14.2. and 14.4.), and are shown in Fig. 8. As indicated above, each sample had two runs; i.e. two elution peaks. For eIF3-Δ60 and eIF3-prt1-1, lanes 1-9 correspond to the consecutive elution fractions of the first run and lanes 10-18 correspond to the consecutive elution fractions of the second run. In case of eIF3-rnp1, where only fractions from the first run were collected, lanes 1-17 correspond to the consecutive elution fraction of the whole elution peak.

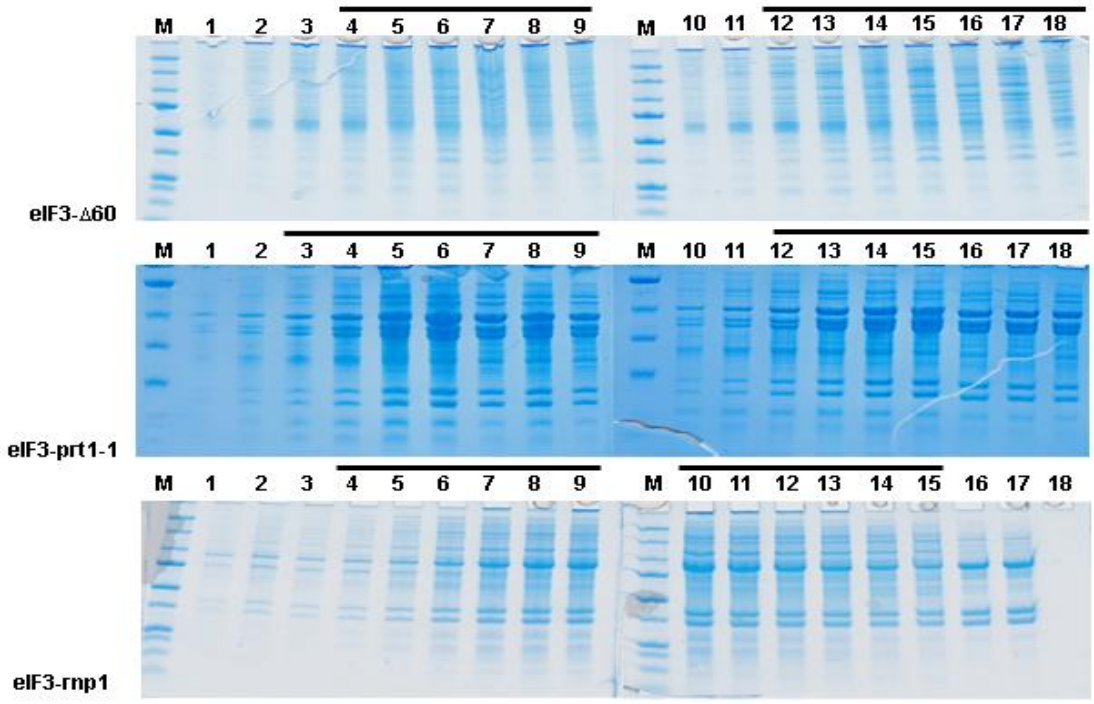

Figure 8. SDS-PAGE analysis of the elution fractions containing mutant eIF3 complexes (eIF3-Δ60, eIF3-prt1-1 and eIF3-rnp1) after a size exclusion column purification step. Fractions marked with the black bar were pooled and applied onto the phosphocellulose column, as a final purification step.

The most protein-rich elution fractions (lanes 4-9 and 12-18 for eIF3-Δ60, lanes 3-9 and 12-18 for eIF3-prt1-1, and lanes 4-15 for eIF3-rnp1 in Fig. 8) were pooled together and loaded onto a freshly prepared 5 mL phosphocellulose column. The capacity of a 5 mL phosphocellulose column was sufficient in this case because I was working with less protein compared to the original protocol. The column was washed and the complexes eluted as described in the corresponding chapter of Material and methods. The resulting fractions were analyzed by SDS-PAGE and are shown in Fig. 9.

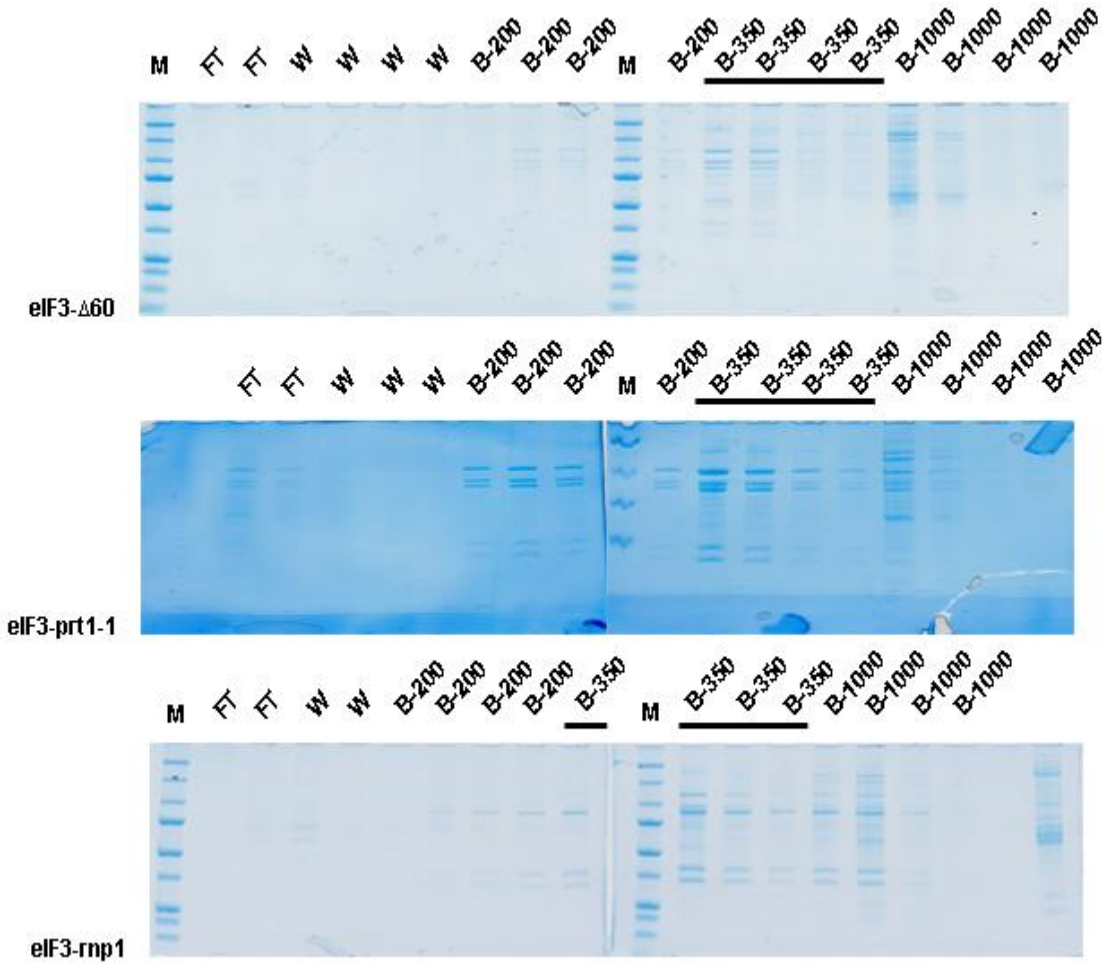

Figure 9. SDS-Page analysis of the elution fractions containing mutant eIF3 complexes (eIF3-Δ60, eIF3-prt1-1 and eIF3-rnp1) after a phosphocellulose column purification step. Fractions marked with the black bar were used further.

The 5 mL fractions from the previous step (elution with the buffer B-350) were pooled together and dialyzed into 2 L enzyme storage buffer over night using 30mL or 15mL dialyses cassettes. The dialyzed samples were then concentrated to the final volume of ~0.5 mL and 20 µL aliquots were flash frozen in liquid nitrogen and stored at -80°C.

Total protein concentrations of mutant eIF3 complexes were determined by Bradford assay (see chapter 15.7.) and are given in Table 4.

Complex	Concentration
eIF3-Δ60	2,07 μM
eIF3-prt1-1	12,5 μM
eIF3-rnp1	7,12 μM

Table 4. Total protein concentration of mutant eIF3 complexes

All purified eIF3 complexes were tested for the presence of contaminating nucleases according to the protocol described in chapter 15.8. in Material and methods. The nuclease contamination could cause mRNA degradation in *in vitro* assays working with RNAs and thus ruin the experiment. In the case of the three purified complexes described here, no contamination with nucleases was detected (data not shown).

20. Effects of *PRT1* and *NIP1* mutations on eIF3 binding to the 40S ribosomes *in vitro*

Lorsch and colleagues previously used the 43S gel shift assay method to monitor efficiency of formation of the 43S complex (Acker et al. 2007, Mitchell et al., 2010). With help of this protocol they showed that wt eIF3 binds tightly to the 40S ribosomes by determining the dissociation constant of eIF3 from the 43S complex to be at Kd=30nM. My first task was thus to determine the binding constant (Kd) for each mutant eIF3 complex, which is described in the following chapters. This parameter is critically needed for setting up the following assays such as the mRNA recruitment assay that should give us an answer to the major question of this work: what eIF3 domains are critically required for this particular process.

20.1. The C-terminal truncation of NIP1 in *nip1-Δ60* does not change the binding affinity of the mutant eIF3 complex to the 43S PIC

The 43S gel shift assay was performed three times according to the protocol (described in chapter 16.) using the final concentrations for both wt and mutant eIF3 complexes ranging from 15 nM to 500 nM. The reduction in mobility of the 43S complex (indicative of a complex formation between eIF3 and the 43S PIC) in a native

gel caused by eIF3 binding was monitored using ^{35}S-Met-tRNA$_i^{Met}$. Upon completion of the assay, the gels containing hot ^{35}S-Met-tRNA$_i^{Met}$ were exposed to an imaging plate BAS cassette 2025 (FUJIFILM) over night and the next day scanned with Molecular Imager FX™ (Bio-Rad). Fig. 10 shows the reduction in mobility of 43S complex caused by eIF3-Δ60 binding. The radio-band shifts already in lanes 2 and 3, where the final concentration 15 nM and 30 nM, respectively, of eIF3-Δ60 was used, indicating that this mutant complex binds 43S PIC as tightly as the wt.

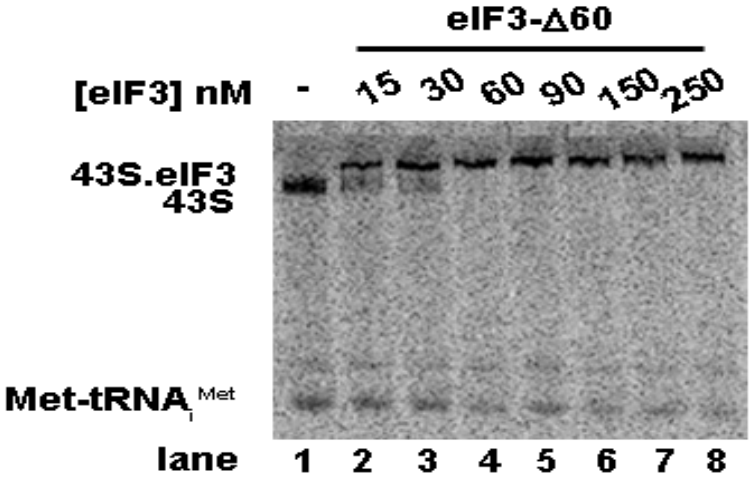

Figure 10. Reduction in mobility of the 43S complex in native gel caused by binding of eIF3-Δ60, monitored using ^{35}S-Met-tRNA$_i^{Met}$

For accurate comparison with the wt complex the quantification was needed and so the resulting gels were analyzed with the ImageJ software. The signal in each lane was expressed as a percentage of the bound state and plotted with help of the Kalaidograf software. The data were then fitted into the binding curves using the Michaelis-Menten equation (($[AB]/[A]_{total}$)=a*[B]/(Kd+[B])). The best fit of my experimental data showed the actual binding constant (Kd) of 14.5±4.7 nM for wt eIF3 and 22.7±5.1 nM for eIF3-Δ60. Since the limiting factor in my experiment was the 40S subunit at the final concentration of 30 nM, the 30 nM value represents a critical threshold for the Kd determination. In other words, any Kd number measured below this threshold is insignificant. This implies that even though the absolute values of the Kd for wt vs. mutant optically differ, they are under the „detection limit“ and the only possible conclusion that I can draw is that the binding affinities of both samples are in average

lower or equal to 30 nM. The eIF3-Δ60 complex thus, in this experimental set-up, does not seem to affect tight binding of eIF3 to the 43S PICs.

20.2. The *PRT1* mutations disrupt the 43S PIC formation

For eIF3 complexes with mutations in the PRT1 subunit (eIF3-prt1-1 and eIF3-rnp1), the 43S gel shift assay (see chapter 16.) was performed using the final concentrations for both wt and mutant eIF3 complexes ranging from 15nM to 750nM. The data analysis was carried essentially the same as above. For the eIF3-prt1-1 mutant complex the actual binding constant was determined to be at 169.25±58.1 nM compared to less than 30nM for wt eIF3. See the original gel in Fig. 11, that clearly shows that eIF3-prt1-1 complex binds to the 43S PIC less tightly (~5-fold) than the wt eIF3.

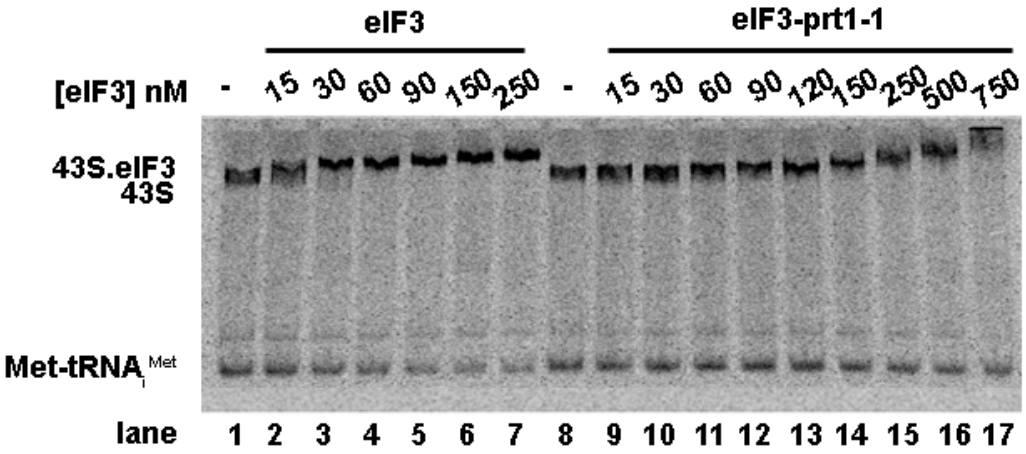

Figure 11. Reduction in mobility of the 43S complex in native gel caused by binding of wt eIF3 (lane 2-7) and eIF3-prt1-1 (lane 9-17), monitored using ^{35}S-Met-tRNA$_i^{Met}$.

I could not analyze the data obtained with the eIF3-rnp1 mutant, because two well distinguishable bands corresponding to the bare and eIF3-bound 43S PICs did not form in these gels (Fig. 12, lane 11-14). In fact, the signal was somewhat shifted up but in a form of a smear starting already at the bottom of the loading well looking as if some complexes got stuck in there and did not get transferred in the gel. Regardless my inability to determine the Kd for the *rnp1* mutants, these gels clearly document that higher concentrations of eIF3-rnp1 disrupt the eIF3 unbound state of the pre-incubated

43S PICs without releasing the radioactively labeled Met-tRNA$_i^{Met}$, however. Under these circumstances, I was indeed not able to test the eIF3-rnp1 mutant complex for its ability to recruit mRNA to the PICs in an *in vitro* mRNA recruitment assay, as described below for the other two mutants.

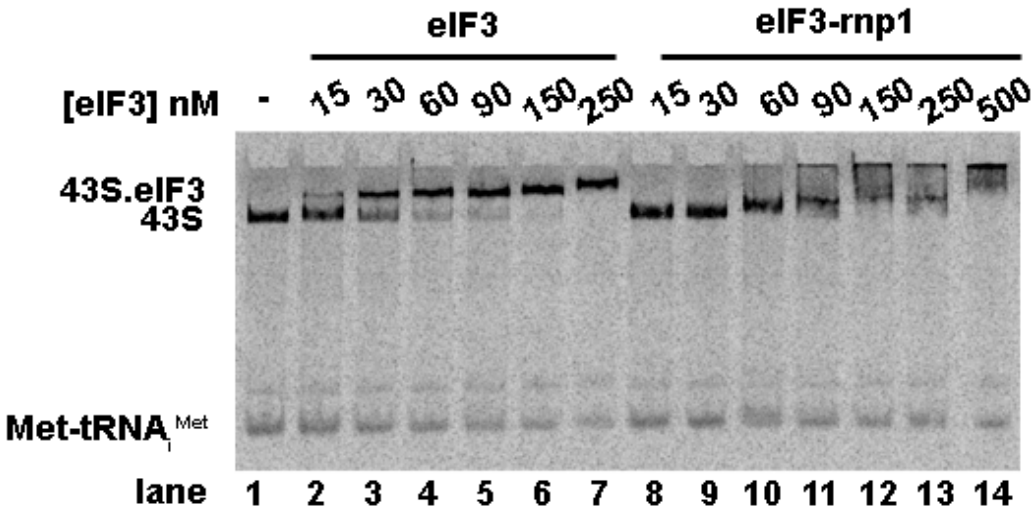

Figure 12. Reduction in mobility of the 43S complex in native gel caused by binding of wt eIF3 (lane 2-7) and eIF3-rnp1 (lane 8-14), monitored using ^{35}S-Met-tRNA$_i^{Met}$.

To conclude, two different mutations in the PRT1 subunit were tested for their ability to associate with the 43S PIC and both showed a significant defect. eIF3-prt1-1 displayed the decreased binding affinity to the 43S PIC (~5-fold) and, in a higher concentration, disturbed the formation of a clear band shift corresponding to eIF3-rnp1 - 43S PIC complex to the same extent as did the eIF3-rnp1 mutation already at lower concentrations.

21. The C-terminal truncation of NIP1 in *nip1-Δ60* does not affect the mRNA recruitment.

Because the 43S PIC dissociation constant of eIF3-Δ60 is similar to wt eIF3, the ultimate mRNA recruitment assay (described in chapter 17.) was performed under the same conditions for both eIF3 complexes at the final concentration of 200nM. This concentration allows full saturation of the 43S complexes by eIF3. The reduction in mobility of free capped *RPL41A* mRNA invoked by its binding to the 43S PIC

(including wt or mutant eIF3) in native gel was monitored using radioactively labeled mRNA (*RPL41A*). The gels containing hot ^{32}P-mRNA were exposed to an imaging plate BAS cassette 2025 (FUJIFILM) for 30 minutes, scanned with Molecular Imager FX™ (Bio-Rad) and analyzed with the ImageJ software. The measured data were fitted into the binding curve using the Exponential Rise equation ($[AB]_t/[AB]_{max}= a*(1-exp(-k_{obs}*t))$).

In the presence of eIF3-Δ60, capped *RPL41A* was recruited to the PIC with an observed rate constant (k_{obs}) of 0.17 min^{-1} and an endpoint of 0.66 corresponding to a fraction of mRNA bound to the PIC (Fig. 13, orange). This rate and endpoint values do not differ in any way from those measured with wt eIF3 under the same conditions (Fig. 13, black). Importantly, my data are perfectly consistent with the already published data for the mRNA recruitment in a presence of wt eIF3, where the observed rate constant was 0.25 min^{-1} (Mitchell et al., 2010). Thus, I conclude that the extreme C-terminal domain of NIP1, which was shown to interact with the small ribosomal protein ASC1 (Kouba et al., 2011), does not seem to affect the mRNA recruitment.

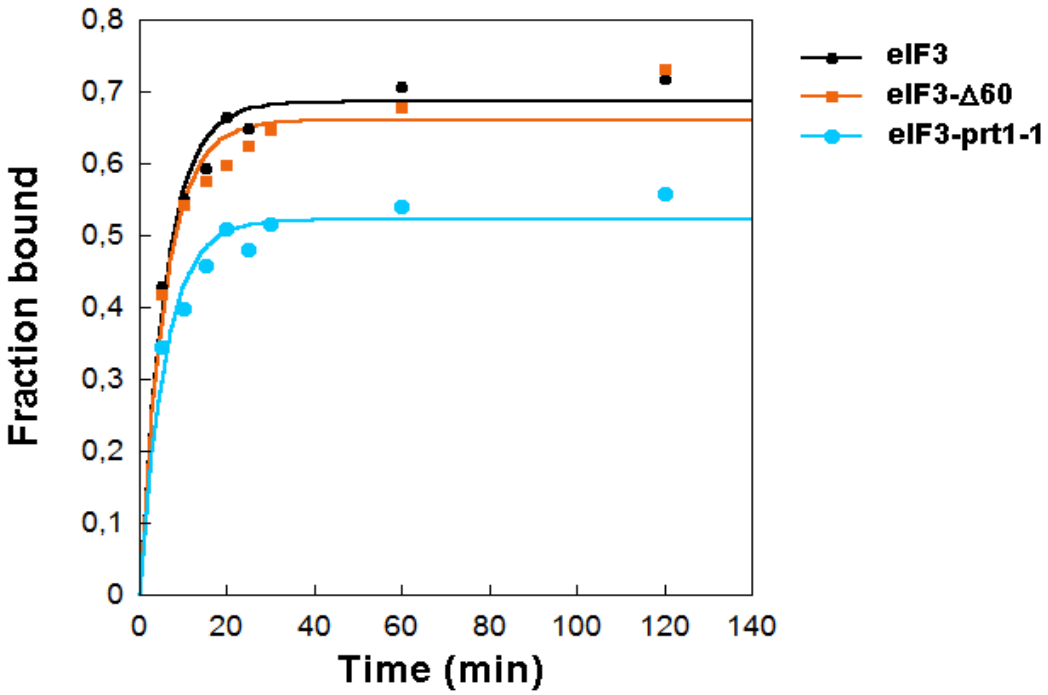

Figure 13. Kinetics of the stable mRNA recruitment to the 43S pre-initiation complex. For cap-*RPL41A*, k_{obs} were determined with eIF3 (black; k_{obs} = 0.17 ± 0.019 min^{-1}), eIF3-Δ 60 (orange; k_{obs} = 0.17 ± 0.026 min^{-1}) and eIF3-prt1-1 (blue; k_{obs} = 0.17 ± 0.025 min^{-1}).

22. The *prt1-1* mutation reduces the efficiency but not the rate of mRNA recruitment to 43S PICs *in vitro*

To saturate the 43S PICs with purified eIF3, it is common to use the concentration that is 10-fold higher than the actual Kd. In the specific case of eIF3-prt1-1 the Kd was determined to be at ~169.25 nM; hence, for the mRNA recruitment assays, I should have used ~1.7 μM concentration of eIF3. However, the 43S gel shift assays revealed that eIF3 concentrations greater than 500nM produced a smear that could not be analyzed further, as aforementioned. Thus, to perform the mRNA recruitment assay with the eIF3-prt1-1 mutant the final concentration of 400nM was used. At this concentration, no 43S PICs in their unbound state were observed in the gel (data not shown) suggesting that the complexes were indeed eIF3-saturated, which was desirable.

In the presence of eIF3-prt1-1, our model *RPL41A* mRNA was recruited to the 43S PIC with an observed rate constant (k_{obs}) of 0.17 min^{-1} and an endpoint of 0.52 (Fig. 13, blue). Hence, whereas the rate of mRNA binding to the PIC remained unchanged in the mutant vs. wt eIF3 (Fig. 13, black), the lower endpoint; i.e. the amount of mRNA stably bound to the 43S PICs, suggests that the efficiency of mRNA recruitment is impaired in the eIF3-prt1-1. Furthermore, the reduction in the amount of mRNAs recruited to the PICs seems to be accompanied by a formation of new, aberrant subcomplexes still capable of mRNA binding (Fig. 14). The composition of these new subcomplexes remains to be identified.

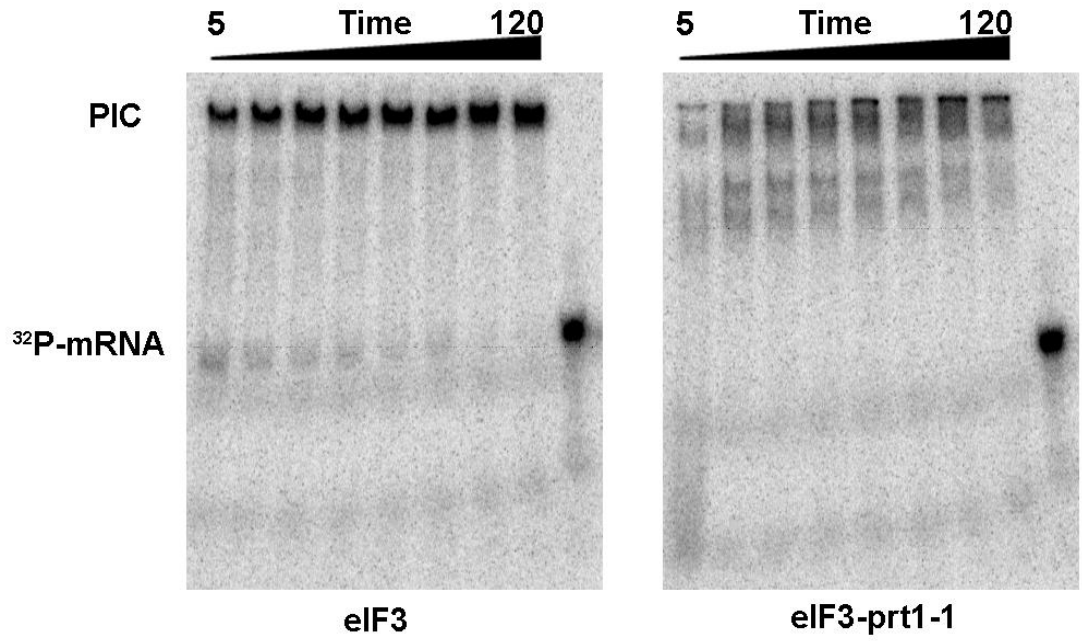

Figure 14. ^{32}P-mRNA (*RPL41A*) gel shift assay showing the effect of wt eIF3 (left) and mutant eIF3-prt1-1 (right) in a presence of saturating concentrations of all factors forming the pre-initiation complex (PIC) in time.

Discussion

The mRNA recruitment is an essential step in protein synthesis and represents one of the major targets of post-transcriptional gene regulation in eukaryotes. Although we know a great deal about what factors are involved in this process, our knowledge of the molecular mechanics of the events that take place during this step is rudimentary.

It was shown recently that, at least in the budding yeast, eIF3 seems to be the key factor in promoting the mRNA recruitment of natural mRNAs to 40S ribosomes *in vivo* and *in vitro* (Mitchell et al., 2010; Jivotovskaya et al., 2006). Although the role for eIF3 in mRNA recruitment has long been known (Trachsel and Staehelin, 1979; Trachsel et al., 1977; Benne and Hershey, 1978), its centrality was not clear back then since it was impossible to disentangle effects on TC recruitment from those on mRNA binding in the old mammalian reconstituted systems, where much of the work on eIF3´s role was originally done (e.g.(Chaudhuri et al., 1999; Kolupaeva et al., 2005)). In other words, eIF3 was shown to have a dramatic effect on the efficiency of the TC recruitment in these systems and since this step precedes mRNA recruitment, it was hard to judge where the observed impact on mRNA recruitment is direct or a consequence of the TC binding defect. Interestingly, whereas the impact of eIF3 on mRNA recruitment in the yeast reconstituted system is huge (Mitchell et al., 2010), the effect of yeast eIF3 on the TC binding is, compared to mammalian systems, relatively small (~2-3 fold) (Algire et al., 2002).

The lack of our knowledge on the eIF3 mechanism of action in promoting the mRNA recruitment inspired me to carry out this Diploma thesis with a major goal to dissect the roles of individual regions of this factor in this important process. For this purpose, I prepared a set of yeast strains overproducing different mutant eIF3 complexes all having a potential to impact the mRNA recruitment step, as could be monitored by the well established *in vitro* mRNA binding assay. Since this is a rather complex, long-term project, analysis of only a few mutations from the complete list is mentioned here.

During the preparation of eIF3 overexpressing strains I noticed two noteworthy facts. Firstly, using covering plasmids with the methionine promoter blocking the expression of a given gene after addition of methionine to the media was ultimately

successful but not as easy as anticipated. Many revertants were produced during the whole procedure for unknown reasons that made me to carefully control each and every sub-step of the preparation. To eliminate this undesirable effect, I tried an alternative approach by deleting individual eIF3 subunits in a diploid strain and obtaining the desired clones by tetrad dissection. However, the diploid cells were defective for sporulation and thus I had to return back to the original strategy. And secondly, all of my newly generated mutant strains grew with slightly slower growth rates when compared to their original genetic backgrounds. The differences in growth between wt cells overexpressing wt eIF3 and individual mutants in high copy were still the same, but all overexpressing strains were slower when compared to the same wt or mutants strains carrying only single gene copies of all subunit. The most feasible explanation of this observation is that it is a direct consequence of the combined effect of deletion of both peptidases and overexpression of all five eIF3 subunits. Mainly the latter must represent a dramatic, extra work-load for the entire expression machinery, where ribosomes seems to be the limiting factor based on recent analysis (Chu et al., 2011).

My *in vitro* measurements then revealed that the 60 amino acid residue C-terminal truncation of NIP1 in *nip1-Δ60* does not affect the mRNA recruitment suggesting that the extreme end of NIP1 is not a factor in the eIF3 role in mRNA recruitment, despite the fact that it is adjacent to the PCI domain shown to possess strong RNA affinity. In fact, Kouba et al. proposed that the initiation defect of the *nip1-Δ60* mutant is caused by a decreased stability of the 43S PIC and/or by a reduced rate of its formation *in vivo* (Kouba et al., 2011). Since no effect on the Kd of the eIF3-Δ60 binding to the 43S PIC was observed it possible that either this *in vitro* assay is less sensitive (lacking some factors) than that used by Kouba *in vivo*, or that the effect of eIF3-Δ60 is more on stability than on the rate of formation. In the latter assay the PICs are subjected to high velocity sedimentation with severe centrifugal forces that may disrupt complexes with weakened stability. Since no such a treatment is required in the *in vitro* assays, no effect can be observed.

Both *PRT1* mutants yielded interesting results in both *in vitro* experiments, however, the quantification of the resulting gels and thus the final interpretation of the data was not straightforward. Both mutations were first tested for their ability to associate with the 43S PIC and both showed a significant defect. At lower concentrations, eIF3-prt1-1 displayed the decreased binding affinity to the 43S PIC

(~5-fold) and in higher concentrations it disturbed the formation of the 43S PICs producing a smear rather than a clear band shift corresponding to the fully formed eIF3-rnp1–43S PIC complex. Luckily, it was still possible to perform the mRNA recruitment assay, in contrast to the eIF3-rnp1 complex that had the same disruptive effect only already at low concentrations, and a clear effect associated with the efficiency of mRNA loading – not with its rate – was observed. It comes in agreement with the earlier data showing that the *prt1-1* mutation does impair mRNA binding to 40S subunits in cell free lysates at the non-permissive temperature (Phan et al., 2001). It is not consistent, however, with later *in vivo* observation that *prt1-1* does not affect the mRNA loading *in vivo* (Nielsen et al., 2004). This repetitive observation of a discrepancy between the *in vitro* and *in vivo* data suggests that there is still something about this mutant that we do not understand and calls for reopening this case to figure out what it is. Interestingly, *prt1-1* shows the effect opposite to that of eIF4G, whose absence in this very system did not affect the amount of mRNA recruited to the 43S PICs but the speed of this process (Mitchell et al., 2010).

It is unfortunate that none of mutants that have been tested so far showed a specific defect in mRNA recruitment without disrupting the 43S PICs at higher concentrations. But the analysis of many more of the eIF3 mutants with more relevant *in vivo* effects is underway that should generate more specific data that will be easier to interpret. Next I plan to use the already purified complexes mentioned here as well as the new ones in other *in vitro* assays that are capable of monitoring the effects of eIF3 mutations in other initiations steps such as scanning and AUG recognition. We believe that this *in vitro* biophysical approached combined with yeast genetics and biochemistry will significantly advance our knowledge of eIF3 role in the entire process of translation initiation.

Conclusion

The major achievements of my work are as follows:

- **Construction of yeast deletion strains overexpressing various mutant eIF3 complexes;**
- **Adaptation of the existing *in vitro* 43S formation and mRNA recruitment assays for tests with mutant eIF3 complexes;**
- **Demonstration that the *nip1*-Δ*60* mutant does not affect either 43S formation/binding or mRNA recruitment;**
- **Demonstration that the *prt1-1* and *prt1-rnp1* mutations of *PRT1* somehow destabilize the 43S PIC when in molar excess and that *prt1-1* impairs efficiency of mRNA recruitment.**

References

Algire, M. A., Maag, D., Savio, P., Acker, M. G., Tarun, S. Z., Sachs, A. B., Asano, K., Nielsen, K. H., Olsen, D. S., Phan, L., et al. (2002). Development and characterization of a reconstituted yeast translation initiation system. RNA (New York, N.Y.) *8*, 382–397.

Asano, K., Clayton, J., Shalev, A., and Hinnebusch, A. G. (2000). A multifactor complex of eukaryotic initiation factors, eIF1, eIF2, eIF3, eIF5, and initiator tRNA(Met) is an important translation initiation intermediate in vivo. Genes & development *14*, 2534–2546.

Asano, K., Phan, L., Anderson, J., and Hinnebusch, A. G. (1998). Complex formation by all five homologues of mammalian translation initiation factor 3 subunits from yeast Saccharomyces cerevisiae. The Journal of biological chemistry *273*, 18573–18585.

Asano, K., Shalev, A., Phan, L., Nielsen, K., Clayton, J., Valásek, L., Donahue, T. F., and Hinnebusch, A. G. (2001). Multiple roles for the C-terminal domain of eIF5 in translation initiation complex assembly and GTPase activation. The EMBO journal *20*, 2326–2337.

Behlke, J., Bommer, U. A., Lutsch, G., Henske, A., and Bielka, H. (1986). Structure of initiation factor eIF-3 from rat liver. Hydrodynamic and electron microscopic investigations. European journal of biochemistry / FEBS *157*, 523–530.

Benne, R., and Hershey, J. W. (1978). The mechanism of action of protein synthesis initiation factors from rabbit reticulocytes. The Journal of biological chemistry *253*, 3078–3087.

Bradford, M. M. (1976). A rapid and sensitive method for the quantitation of microgram quantities of protein utilizing the principle of protein-dye binding. Analytical biochemistry *72*, 248–254.

Chaudhuri, J., Chowdhury, D., and Maitra, U. (1999). Distinct functions of eukaryotic translation initiation factors eIF1A and eIF3 in the formation of the 40 S ribosomal preinitiation complex. The Journal of biological chemistry *274*, 17975–17980.

Chiu, W.-L., Wagner, S., Herrmannová, A., Burela, L., Zhang, F., Saini, A. K., Valásek, L., and Hinnebusch, A. G. (2010). The C-terminal region of eukaryotic translation initiation factor 3a (eIF3a) promotes mRNA recruitment, scanning, and, together with eIF3j and the eIF3b RNA recognition motif, selection of AUG start codons. Molecular and cellular biology *30*, 4415–4434.

Chu, D., Barnes, D. J., and von der Haar, T. (2011). The role of tRNA and ribosome competition in coupling the expression of different mRNAs in Saccharomyces cerevisiae. Nucleic acids research *39*, 6705–6714.

Cuchalová, L., Kouba, T., Herrmannová, A., Dányi, I., Chiu, W.-L., and Valásek, L. (2010). The RNA recognition motif of eukaryotic translation initiation factor 3g (eIF3g) is required for resumption of scanning of posttermination ribosomes for reinitiation on GCN4 and together with eIF3i stimulates linear scanning. Molecular and cellular biology *30*, 4671–4686.

Damoc, E., Fraser, C. S., Zhou, M., Videler, H., Mayeur, G. L., Hershey, J. W. B., Doudna, J. a, Robinson, C. V., and Leary, J. a (2007). Structural characterization of the human eukaryotic initiation factor 3 protein complex by mass spectrometry. Molecular & cellular proteomics : MCP *6*, 1135–1146.

Danaie, P., Wittmer, B., Altmann, M., and Trachsel, H. (1995). Isolation of a protein complex containing translation initiation factor Prt1 from Saccharomyces cerevisiae. The Journal of biological chemistry *270*, 4288–4292.

Deo, R. C., Bonanno, J. B., Sonenberg, N., and Burley, S. K. (1999). Recognition of polyadenylate RNA by the poly(A)-binding protein. Cell *98*, 835–845.

Dmitriev, S. E., Terenin, I. M., Dunaevsky, Y. E., Merrick, W. C., and Shatsky, I. N. (2003). Assembly of 48S translation initiation complexes from purified components with mRNAs that have some base pairing within their 5' untranslated regions. Molecular and cellular biology *23*, 8925–8933.

ElAntak, L., Tzakos, A. G., Locker, N., and Lukavsky, P. J. (2007). Structure of eIF3b RNA recognition motif and its interaction with eIF3j: structural insights into the recruitment of eIF3b to the 40 S ribosomal subunit. The Journal of biological chemistry *282*, 8165–8174.

Elantak, L., Wagner, S., Herrmannová, A., Karásková, M., Rutkai, E., Lukavsky, P. J., and Valásek, L. (2010). The indispensable N-terminal half of eIF3j/HCR1 cooperates with its structurally conserved binding partner eIF3b/PRT1-RRM and with eIF1A in stringent AUG selection. Journal of molecular biology *396*, 1097–1116.

Fabian, J. R., Kimball, S. R., Heinzinger, N. K., and Jefferson, L. S. (1997). Subunit assembly and guanine nucleotide exchange activity of eukaryotic initiation factor-2B expressed in Sf9 cells. The Journal of biological chemistry *272*, 12359–12365.

Fraser, C. S., Lee, J. Y., Mayeur, G. L., Bushell, M., Doudna, J. A., and Hershey, J. W. (2004). The j-subunit of human translation initiation factor eIF3 is required for the stable binding of eIF3 and its subcomplexes to 40S ribosomal subunits in vitro. J Biol Chem *279*, 8946–8956.

Guo, J., Hui, D. J., Merrick, W. C., and Sen, G. C. (2000). A new pathway of translational regulation mediated by eukaryotic initiation factor 3. The EMBO journal *19*, 6891–6899.

Harris, T. E., Chi, A., Shabanowitz, J., Hunt, D. F., Rhoads, R. E., and Lawrence, J. C. (2006). mTOR-dependent stimulation of the association of eIF4G and eIF3 by insulin. The EMBO journal *25*, 1659–1668.

Hartwell, L. H., and McLaughlin, C. S. (1968). Temperature-sensitive mutants of yeast exhibiting a rapid inhibition of protein synthesis. Journal of bacteriology *96*, 1664–1671.

Herrmannová, A., Daujotyte, D., Yang, J.-C., Cuchalová, L., Gorrec, F., Wagner, S., Dányi, I., Lukavsky, P. J., and Shivaya Valásek, L. (2011). Structural analysis of an eIF3 subcomplex reveals conserved interactions required for a stable and proper translation pre-initiation complex assembly. Nucleic acids research.

Holz, M. K., Ballif, B. A., Gygi, S. P., and Blenis, J. (2005). mTOR and S6K1 mediate assembly of the translation preinitiation complex through dynamic protein interchange and ordered phosphorylation events. Cell *123*, 569–580.

Isken, O., Kim, Y. K., Hosoda, N., Mayeur, G. L., Hershey, J. W. B., and Maquat, L. E. (2008). Upf1 phosphorylation triggers translational repression during nonsense-mediated mRNA decay. Cell *133*, 314–327.

Jackson, R. J., Hellen, C. U. T., and Pestova, T. V. (2010). The mechanism of eukaryotic translation initiation and principles of its regulation. Nat Rev Mol Cell Biol *11*, 113–127.

Jirincová, H., Vavricková, P., Palecek, J., and Hasek, J. (1998). A new monoclonal antibody against Rpg1p. Folia biologica *44*, 73.

Jivotovskaya, A. V., Valásek, L., Hinnebusch, A. G., and Nielsen, K. H. (2006). Eukaryotic translation initiation factor 3 (eIF3) and eIF2 can promote mRNA binding to 40S subunits independently of eIF4G in yeast. Molecular and cellular biology *26*, 1355–1372.

Jäger, S., Cimermancic, P., Gulbahce, N., Johnson, J. R., McGovern, K. E., Clarke, S. C., Shales, M., Mercenne, G., Pache, L., Li, K., et al. (2012). Global landscape of HIV-human protein complexes. Nature *481*, 365–370.

Keierleber, C., Wittekind, M., Qin, S. L., and McLaughlin, C. S. (1986). Isolation and characterization of PRT1, a gene required for the initiation of protein biosynthesis in Saccharomyces cerevisiae. Molecular and cellular biology *6*, 4419–4424.

Khoshnevis, S., Neumann, P., and Ficner, R. (2010). Crystal structure of the RNA recognition motif of yeast translation initiation factor eIF3b reveals differences to human eIF3b. PloS one *5*.

Kolupaeva, V. G., Unbehaun, A., Lomakin, I. B., Hellen, C. U. T., and Pestova, T. V. (2005). Binding of eukaryotic initiation factor 3 to ribosomal 40S subunits and its role in ribosomal dissociation and anti-association. RNA (New York, N.Y.) *11*, 470–486.

Kouba, T., Rutkai, E., Karásková, M., and Valásek, L. S. (2011). The eIF3c/NIP1 PCI domain interacts with RNA and RACK1/ASC1 and promotes assembly of translation preinitiation complexes. Nucleic acids research, 1–17.

Krishnamoorthy, T., Pavitt, G. D., Zhang, F., Dever, T. E., and Hinnebusch, A. G. (2001). Tight binding of the phosphorylated alpha subunit of initiation factor 2 (eIF2alpha) to the regulatory subunits of guanine nucleotide exchange factor eIF2B is required for inhibition of translation initiation. Molecular and cellular biology *21*, 5018–5030.

LeFebvre, A. K., Korneeva, N. L., Trutschl, M., Cvek, U., Duzan, R. D., Bradley, C. A., Hershey, J. W. B., and Rhoads, R. E. (2006). Translation initiation factor eIF4G-1 binds to eIF3 through the eIF3e subunit. The Journal of biological chemistry *281*, 22917–22932.

Marintchev, A., and Wagner, G. Translation initiation: structures, mechanisms and evolution. Quarterly reviews of biophysics *37*, 197–284.

Marintchev, A., and Wagner, G. Translation initiation: structures, mechanisms and evolution. Quarterly reviews of biophysics *37*, 197–284.

Masutani, M., Sonenberg, N., Yokoyama, S., and Imataka, H. (2007). Reconstitution reveals the functional core of mammalian eIF3. EMBO Journal *26*, 3373–3383.

Mitchell, S. F., Walker, S. E., Algire, M. A., Park, E.-H., Hinnebusch, A. G., and Lorsch, J. R. (2010). The 5'-7-methylguanosine cap on eukaryotic mRNAs serves both to stimulate canonical translation initiation and to block an alternative pathway. Molecular cell *39*, 950–962.

Munzarová, V., Pánek, J., Gunišová, S., Dányi, I., Szamecz, B., and Valášek, L. S. (2011). Translation reinitiation relies on the interaction between eIF3a/TIF32 and progressively folded cis-acting mRNA elements preceding short uORFs. PLoS genetics *7*, e1002137.

Méthot, N., Song, M. S., and Sonenberg, N. (1996). A region rich in aspartic acid, arginine, tyrosine, and glycine (DRYG) mediates eukaryotic initiation factor 4B (eIF4B) self-association and interaction with eIF3. Molecular and cellular biology *16*, 5328–5334.

Naranda, T., MacMillan, S. E., and Hershey, J. W. (1994). Purified yeast translational initiation factor eIF-3 is an RNA-binding protein complex that contains the PRT1 protein. The Journal of biological chemistry *269*, 32286–32292.

Nielsen, K. H., Szamecz, B., Valásek, L., Jivotovskaya, A., Shin, B.-S., and Hinnebusch, A. G. (2004). Functions of eIF3 downstream of 48S assembly impact AUG recognition and GCN4 translational control. The EMBO journal *23*, 1166–1177.

Nielsen, K. H., Valásek, L., Sykes, C., Jivotovskaya, A., and Hinnebusch, A. G. (2006). Interaction of the RNP1 motif in PRT1 with HCR1 promotes 40S binding of eukaryotic initiation factor 3 in yeast. Molecular and cellular biology *26*, 2984–2998.

Park, H. S., Himmelbach, A., Browning, K. S., Hohn, T., and Ryabova, L. A. (2001). A plant viral "reinitiation" factor interacts with the host translational machinery. Cell *106*, 723–733.

Passmore, L. A., Schmeing, T. M., Maag, D., Applefield, D. J., Acker, M. G., Algire, M. A., Lorsch, J. R., and Ramakrishnan, V. (2007). The eukaryotic translation initiation factors eIF1 and eIF1A induce an open conformation of the 40S ribosome. Molecular cell *26*, 41–50.

Pavitt, G. D., Ramaiah, K. V., Kimball, S. R., and Hinnebusch, A. G. (1998). eIF2 independently binds two distinct eIF2B subcomplexes that catalyze and regulate guanine-nucleotide exchange. Genes & development *12*, 514–526.

Pestova, T. V., Lomakin, I. B., Lee, J. H., Choi, S. K., Dever, T. E., and Hellen, C. U. (2000). The joining of ribosomal subunits in eukaryotes requires eIF5B. Nature *403*, 332–335.

Phan, L., Schoenfeld, L. W., Valásek, L., Nielsen, K. H., and Hinnebusch, a G. (2001). A subcomplex of three eIF3 subunits binds eIF1 and eIF5 and stimulates ribosome binding of mRNA and tRNA(i)Met. The EMBO journal *20*, 2954–2965.

Phan, L., Zhang, X., Asano, K., Anderson, J., Vornlocher, H. P., Greenberg, J. R., Qin, J., and Hinnebusch, A. G. (1998). Identification of a translation initiation factor 3 (eIF3) core complex, conserved in yeast and mammals, that interacts with eIF5. Mol Cell Biol *18*, 4935–4946.

Pisarev, A. V., Kolupaeva, V. G., Yusupov, M. M., Hellen, C. U. T., and Pestova, T. V. (2008). Ribosomal position and contacts of mRNA in eukaryotic translation initiation complexes. The EMBO journal *27*, 1609–1621.

Pöyry, T. A. A., Kaminski, A., Connell, E. J., Fraser, C. S., and Jackson, R. J. (2007). The mechanism of an exceptional case of reinitiation after translation of a long ORF reveals why such events do not generally occur in mammalian mRNA translation. Genes & development *21*, 3149–3162.

Sachs, A. B., and Varani, G. (2000). Eukaryotic translation initiation: there are (at least) two sides to every story. Nature structural biology *7*, 356–361.

Siridechadilok, B., Fraser, C. S., Hall, R. J., Doudna, J. A., and Nogales, E. (2005). Structural roles for human translation factor eIF3 in initiation of protein synthesis. Science (New York, N.Y.) *310*, 1513–1515.

Szamecz, B., Rutkai, E., Cuchalová, L., Munzarová, V., Herrmannová, A., Nielsen, K. H., Burela, L., Hinnebusch, A. G., and Valásek, L. (2008). eIF3a cooperates with sequences 5' of uORF1 to promote resumption of scanning by post-termination ribosomes for reinitiation on GCN4 mRNA. Genes & development *22*, 2414–2425.

Trachsel, H., Erni, B., Schreier, M. H., and Staehelin, T. (1977). Initiation of mammalian protein synthesis. II. The assembly of the initiation complex with purified initiation factors. Journal of molecular biology *116*, 755–767.

Trachsel, H., and Staehelin, T. (1979). Initiation of mammalian protein synthesis. The multiple functions of the initiation factor eIF-3. Biochimica et biophysica acta *565*, 305–314.

Unbehaun, A., Borukhov, S. I., Hellen, C. U. T., and Pestova, T. V. (2004). Release of initiation factors from 48S complexes during ribosomal subunit joining and the link between establishment of codon-anticodon base-pairing and hydrolysis of eIF2-bound GTP. Genes & development *18*, 3078–3093.

Valásek, L., Phan, L., Schoenfeld, L. W., Valásková, V., and Hinnebusch, a G. (2001). Related eIF3 subunits TIF32 and HCR1 interact with an RNA recognition motif in PRT1 required for eIF3 integrity and ribosome binding. The EMBO journal *20*, 891–904.

Valášek, L., Mathew, A., Shin, B. S., Nielsen, K. H., Szamecz, B., and Hinnebusch, A. G. (2003). The yeast eIF3 subunits TIF32/a, NIP1/c, and eIF5 make critical connections with the 40S ribosome in vivo. Genes & development *17*, 786–799.

Valášek, L., Nielsen, K. H., Zhang, F., Fekete, C. A., and Hinnebusch, A. G. (2004). Interactions of Eukaryotic Translation Initiation Factor 3 (eIF3) Subunit NIP1/c with eIF1 and eIF5 Promote Preinitiation Complex Assembly and Regulate Start Codon Selection. Mol. Cell. Biol. *24*, 9437–9455.

Valášek, L., Nielsen, K. H., and Hinnebusch, A. G. (2002). Direct eIF2-eIF3 contact in the multifactor complex is important for translation initiation in vivo. The EMBO journal *21*, 5886–5898.

Yamamoto, Y., Singh, C. R., Marintchev, A., Hall, N. S., Hannig, E. M., Wagner, G., and Asano, K. (2005). The eukaryotic initiation factor (eIF) 5 HEAT domain mediates multifactor assembly and scanning with distinct interfaces to eIF1, eIF2, eIF3, and eIF4G. Proceedings of the National Academy of Sciences of the United States of America *102*, 16164–16169.

Zhou, M., Sandercock, A. M., Fraser, C. S., Ridlova, G., Stephens, E., Schenauer, M. R., Yokoi-Fong, T., Barsky, D., Leary, J. A., Hershey, J. W., et al. (2008). Mass spectrometry reveals modularity and a complete subunit interaction map of the eukaryotic translation factor eIF3. Proceedings of the National Academy of Sciences of the United States of America *105*, 18139–18144.